ACADEMIC PRESS

Available online at www.sciencedirect.com

SCIENCE DIRECT®

Journal of Sound and Vibration 264 (2003) 1–35

JOURNAL OF SOUND AND VIBRATION

www.elsevier.com/locate/jsvi

Improvement of the semi-analytical method, based on Hamilton's principle and spectral analysis, for determination of the geometrically non-linear response of thin straight structures. Part III: steady state periodic forced response of rectangular plates

M. El Kadiri*, R. Benamar

Laboratoire d'Etudes et de Recherches en Simulation, Instrumentation et Mesures, E.G.T. E.M.I., Université Mohammed V, BP 765 Agdal, Rabat, Morocco

Received 21 September 2001; accepted 26 March 2002

Abstract

In Parts I and II of this series of papers, a practical simple "multi-mode theory", based on the linearization of the non-linear algebraic equations, written on the modal basis, in the neighbourhood of each resonance, has been developed for beams and fully clamped rectangular plates.[1] Simple explicit formulae have been derived, which allowed, via the so-called first formulation, direct calculation of the basic function contributions to the first three non-linear mode shapes of clamped–clamped and clamped–simply supported beams, and the two first non-linear mode shapes of FCRP. Also, in Part I of this series of papers, this approach has been successively extended, in order to determine the amplitude-dependent deflection shapes associated with the non-linear steady state periodic forced response[2] of clamped–clamped beams, excited by a concentrated or a distributed harmonic force in the neighbourhood of the first resonance.

This new approach has been applied in the present work to obtain the NLSSPFR formulation for FCRP, SSRP, and CCCSSRP, leading in each case to a non-linear system of coupled differential equations, which may be considered as a multi-dimensional form of the well-known Duffing equation. The single-mode assumption, and the harmonic balance method, have been used for both harmonic concentrated and distributed excitation forces, leading to one-dimensional non-linear frequency response functions of the plates considered. Comparisons have been made between the curves based on these functions, and the

*Corresponding author.

[1] In the remainder of this paper, both "fully clamped rectangular plates" and "fully clamped rectangular plate" will be denoted as FCRP, depending on the context, as in Ref. [10]. Simply supported rectangular plates will be denoted as SSRP, and clamped–clamped–clamped simply supported rectangular plates as CCCSSRP.

[2] Non-linear steady state periodic forced response is denoted in what follows as NLSSPFR.

0022-460X/03/$ - see front matter
doi:10.1016/S0022-460X(02)01162-8

results available in the literature, showing a reasonable agreement, for finite but relatively small vibration amplitudes. A more accurate estimation of the FCRP non-linear frequency response functions has been obtained by the extension of the improved version of the semi-analytical model developed in Part I for the NLSSPFR of beams, to the case of FCRP, leading to explicit analytical expressions for the "multi-dimensional non-linear frequency response function", depending on the forcing level, and the amplitude of the response induced in the range considered for the excitation frequency.

1. Introduction

The problem of plates vibration is of a continuing interest, due to their frequent use as structural components, especially in aerospace [1]. The geometrically non-linear behaviour of plates is encountered in many recent applications, in which aircraft panels are subjected to high excitation levels, due to the engine jet, or to the atmospheric turbulence, which may exceed 120 dB. In such situations, linear theories fail in predicting deflections, strains, stresses and frequencies [2]. The prediction of service fatigue life is based on r.m.s stress/strain, and predominant response frequency, in conjunction with the stress versus cycles to failure (S–N) data. Current analytical design methods for sonic fatigue prevention are based essentially on linear theory. The use of linear analyses, as mentioned in the above reference, would lead to poor estimation of panel fatigue life. Therefore, it is of crucial interest to develop practical non-linear approaches, allowing the effect of the geometrical non-linearity, due to large displacement amplitudes, to be taken into account in the design process.

In a previous series of papers [3–8], a semi-analytical model has been developed for non-linear free vibrations of thin structures such as beams, plates, and shells. The non-linear vibration problem was reduced to the iterative solution of a set of non-linear algebraic equations, which allows the amplitude-dependent non-linear frequencies and mode shapes of the structure considered to be determined. More recently, this model has been extended to the NLSSPFR of beams [9,10]. The main feature of this approach is that it makes the geometrically non-linear effects appear not only via the amplitude frequency dependence, which was the main concern of most of the previous studies, but also via the dependence of the structure deflection shapes on the amplitude of vibration [3–13]. This allows quantitative estimates of curvatures to be obtained, with the associated non-linear stresses, in sensible regions of the structure, which may be of crucial importance in the fatigue life prediction of structures working in a severe environment. The problem of non-linear forced vibrations of rectangular plates has not been yet examined using the semi-analytical approach described above, neither in its general formulation which was applied to beams in Refs. [9,10], nor in its improved simplified form which was applied to the NLSSPFR of beams in Ref. [11], and to the free response of FCRP in Ref. [12]. The purpose of the present paper is the extension of the models developed previously, to some rectangular plate cases which are excited by concentrated, or distributed harmonic forces, in order to derive the corresponding multi-dimensional Duffing equation. The procedure for solution of the multi-mode model is then discussed, and two degrees of approximations are proposed. The first approximation is based on the single-mode approach, which takes into account the contribution of the first mode, in the modal functions basis defined in Ref. [12], and denoted as the MFB, and neglects the other modal

function contributions. However, as the single-mode approach does not lead to any information concerning the deflection shapes amplitude dependence, which is of crucial importance for determining the associated non-linear curvatures, and non-linear stress patterns, an improved simplified approach, similar to that applied to beams in Ref. [11], is developed in order to obtain an explicit direct solution of the multi-mode model, for the NLSSPFR of FCRP, which is expected to be very useful in further analytical developments, and also for engineering purposes. This assumes, in the light of the numerical results previously obtained for FCRP in Ref. [12], that the higher modal function contributions are not equal to zero, as in the single-mode approach, but are small compared to the first modal function contribution. Then, by neglecting first and second order terms in the system of non-linear algebraic equations, an explicit analytical solution is obtained for the higher modal function contributions to the NLSSPFR of the rectangular plate considered.

In the Section 2, a brief review of the general theory mentioned above is first presented for the case of free vibrations, in order to introduce the notation and the basic concepts. Then, the model is generalized in Section 3 to the NLSSPFR of FCRP. In Section 4, the solution of the multi-dimensional Duffing equation, based on the harmonic balance method and the single-mode approach, is given for various plate aspect ratios, various type of harmonic excitation, i.e., concentrated or distributed, and various levels of excitation. Also, a simplified theory for the solution of the multi-mode model is presented, leading to analytical expressions for the higher modal function contributions. The numerical results obtained, based on the two simplified approaches mentioned above are then compared with previously published results, obtained by other methods, such as the FEM, the HFEM, and the ANM.

2. A brief review of the theoretical formulation, based on Lagrange's equations, for the geometrically non-linear free response of FCRP

2.1. Introduction

The theoretical model based on Hamilton's principle and spectral analysis, successfully used in previous works to determine the non-linear mode shapes of beams, plates and shells [3–8], is used here in order to determine the NLSSPFR of FCRP excited by concentrated or distributed harmonic forces. As an introduction to Section 3, in which the model for the forced case is presented, this section starts by giving a brief review of the theory developed in Refs [3–5] for the free vibration case, in order to make it easy to the reader to understand the notation and the analytical developments presented in the remainder of the paper. Also, the non-linear frequency dependence on the amplitude of vibration, obtained via an exact elliptical solution of the non-linear algebraic system, considered in the case of a single-mode approach, is given for some plate cases and compared with other approximate solutions, previously published.

2.2. General model for non-linear free vibration of FCRP

Consider transverse vibrations of the plate shown in Fig. 1, having the characteristics given in Appendix D. For such a plate, the strain energy V is given as the sum of the strain energy due to

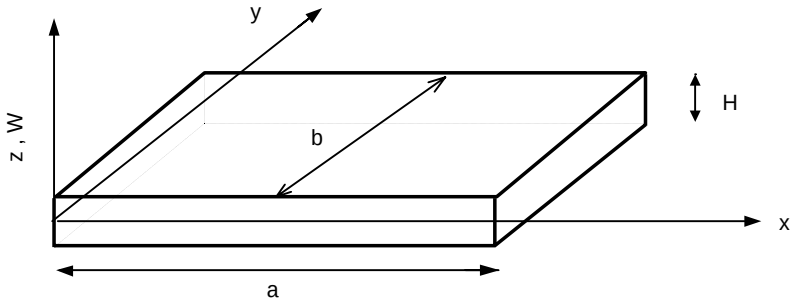

Fig. 1. Plate notation.

the bending V_b, and the membrane strain energy induced by large deflections V_a. In Ref. [5,7], the expressions used for V_b, V_a, and the kinetic energy T have been extensively discussed on the basis of a systematic comparison of the results obtained previously both experimentally and theoretically, based on various approaches. The approximate expressions adopted were

$$V_b = \frac{1}{2}\int_S D\left(\frac{\partial^2 W}{\partial x^2} + \frac{\partial^2 W}{\partial y^2}\right)^2 \mathrm{d}S, \tag{1}$$

$$V_a = \frac{3D}{2H^2}\int_S \left(\left(\frac{\partial W}{\partial x}\right)^2 + \left(\frac{\partial W}{\partial y}\right)^2\right)^2 \mathrm{d}S, \tag{2}$$

$$T = \tfrac{1}{2}\rho H \int_S \left(\frac{\partial W}{\partial t}\right)^2 \mathrm{d}S \tag{3}$$

in which W is the transverse deflection function, and S the plate area. The expression for V_b is the plate simplified bending strain energy expression, valid for the fully clamped boundaries considered in Section 5.2 [14]. For the other boundaries cases, the general expression is given in Appendix A. In all of the above expressions, terms involving the in-plane displacements U and V and their partial derivatives have been omitted, as in Refs. [5,7]. In addition to the discussions given in the above references for justifying such an assumption, the agreement found in the present paper between the results obtained in the non-linear forced case, and those based on other approaches, which are discussed in Section 4.4.2 confirms the validity of such an assumption for reasonable ranges of vibration amplitudes. Assuming that the transverse displacement of a point (x,y) of the plate mid-plane can be written as

$$W(x, y, t) = q_k(t) w_k(x, y) \tag{4}$$

in which the repeated index k is summed over the range $\{1, \ldots, n\}$, n being the number of basic functions w_k used. Substituting W in expressions (1)–(3) for V_b, V_a, T and rearranging leads to

$$V_b = \tfrac{1}{2} q_i q_j k_{ij}, \tag{5}$$

$$V_a = \tfrac{1}{2} q_i q_j q_k q_l b_{ijkl}, \tag{6}$$

$$T = \tfrac{1}{2} \dot{q}_i \dot{q}_j m_{ij} \tag{7}$$

in which m_{ij}, k_{ij} and b_{ijkl} are the general terms of the mass tensor, the rigidity tensor, and the non-linear rigidity tensor defined in Refs. [3,5], and reproduced here in Appendix A. The indices i, j, k and l are summed over 1, …, n.

The dynamic behaviour of the structure may be obtained by Lagrange's equations for a conservative system, which leads after calculation to

$$\ddot{q}_i m_{ir} + q_i k_{ir} + 2q_i q_j q_k b_{ijkr} = 0, \quad r = 1, ..., n. \tag{8}$$

Using matrix notation, and the non-dimensional parameters defined in Ref. [5], and given in Appendix A, system (8) can be written as

$$\left[\mathbf{M}^*\right]\{\mathbf{q}_{\tau\tau}\} + \left[\mathbf{K}^*\right]\{\mathbf{q}\} + 2\left[\mathbf{B}^*(\{\mathbf{q}\})\right]\{\mathbf{q}\} = \{\mathbf{0}\} \tag{9}$$

in which $\{\mathbf{q}_{\tau\tau}\}$ denotes the second derivative of the column vector of generalized co-ordinates $\{\mathbf{q}\}^{\mathrm{T}} = [q_1 q_2 ... q_n]$ with respect to the non-dimensional time parameter $\tau = \omega t$. If harmonic motion is assumed, as in Refs. [5,7], one can write

$$q_k(t) = a_k \sin \omega t \quad \text{and} \quad W(x, y, t) = w(x, y) \sin \omega t = H a_k w_k^*(x^*, y^*) \sin \omega t. \tag{10}$$

Substituting Eq. (10) into Eq. (9) and applying the harmonic balance method leads to

$$\left(\left[\mathbf{K}^*\right] - \omega^{*2}\left[\mathbf{M}^*\right]\right)\{\mathbf{A}\} + \tfrac{3}{2}\left[\mathbf{B}^*(\mathbf{A})\right]\{\mathbf{A}\} = \{\mathbf{0}\} \tag{11}$$

in which $\{\mathbf{A}\}$ is the column vector of basic function contribution coefficients $\{\mathbf{A}\}^{\mathrm{T}} = [a_1 a_2 \ldots a_n]$. Using the tensor notation, the above system may be written as

$$-\omega^{*2} a_i m_{ir}^* + a_i k_{ir}^* + \tfrac{3}{2} a_i a_j a_k b_{ijkr}^* = 0, \quad r = 1 - n. \tag{12}$$

The formulation was completed in Refs. [5,7] by replacing ω^{*2} by its expression obtained from the principle of conservation of energy, i.e.,

$$\omega^{*2} = \frac{a_i a_j k_{ij}^* + a_i a_j a_k a_l b_{ijkl}^*}{a_i a_j m_{ij}^*}. \tag{13}$$

Using a procedure similar to that adopted in many previous works [4,5,7,8,15–18], the contribution of the predominant basic function participating in the non-linear mode shape considered was fixed, and the other basic function contributions were calculated via numerical solution of the remaining (n-1) non-linear algebraic equations.

2.3. Simplified multi-mode approaches for solution of the multi-mode model for geometrically non-linear free vibrations of FCRP

The purpose of this subsection is to give a brief review of the first formulation presented in Part II of this series of papers [12], for free vibration analysis of FCRP.

Consider large vibration amplitudes of a FCRP, having an aspect ratio $\alpha = b/a$ less than 1, in the neighbourhood of its first resonant frequency. Following the choice of basic functions adopted in Ref. [5], the plate deflections in the x and y directions are represented by clamped-clamped beam functions. So, the simple index k of the contribution a_k used in the series expansion (10) for the plate deflection function w_k^* may be replaced by a double index a_{ij}, which means that the plate function w_k^* is the product of the ith and jth clamped–clamped beam functions in the x and y directions, respectively. To determine the first non-linear mode shape of FCRP, the linear rigidity

tensor k^*_{ij} and non-linear geometrical rigidity tensor b^*_{ijkl} have been calculated using the first nine symmetric–symmetric plate basic functions, obtained as products of the first three symmetric clamped–clamped beam mode shapes , in the x and y directions.

The first formulation is based on an approximation which assumes that the contribution vector $\{A\}^T = [a_1 ... a_n]$ can be written as $[a_1 \varepsilon_2 ... \varepsilon_n]$, with ε_i small compared to a_1, for $i = 2$—n. Then, considering the expression $a_i a_j a_k b^*_{ijkr}$ of Eq. (12) which involves summation for the repeated indices i, j, k over the range $\{1,2,\ldots,n\}$, both first and second order terms with respect to ε_i, i.e., terms of the type $a_1^2 \varepsilon_k b^*_{11kr}$, or of the type $a_1 \varepsilon_j \varepsilon_k b^*_{1jkr}$, are neglected. Therefore, the only remaining term is $a_1^3 b^*_{111r}$.

If k^*_{ir}, for $i \neq r$, is assumed to be negligible compared to k^*_{rr}, with the objective of obtaining a direct solution, system (12) permits the basic function contributions ε_2, ε_3,.., ε_9 of the second and higher functions to be obtained explicitly, corresponding to a given value of the assigned first basic function contribution a_1, as follows

$$\varepsilon_r = -\frac{\frac{3}{2} a_1^3 b^*_{111r}}{k^*_{rr} - \omega^{*2} m^*_{rr}} \quad (r = 2, 3, ..., 9). \tag{14}$$

In Part II of this series of papers [12], it was shown that since the BFB does not lead to a diagonal rigidity matrix, application of the above formulation in this basis leads to poor results, and consequently, the problem has been reconsidered in the modal function basis, denoted as MFB.

To reformulate the problem in MFB, the expansion of the transverse displacement function $w^*(x^*, y^*)$ in the form of the finite series: $w^*(x^*, y^*) = a_k w^*_k(x^*, y^*)$, given in Eq. (10), is rewritten as $w^*(x^*, y^*) = \bar{a}_k \phi^*_k(x^*, y^*)$. In the two above expressions, a summation is performed for the index k over the range $\{1,\ldots,n\}$. $\phi^*_k(x^*, y^*)$ is the kth symmetric-symmetric FCRP linear mode shape. These SSFCRP linear mode shapes were obtained by numerical solution of a linear eigenvalue problem, similar to that defined by Eq. (34) of Ref. [12]. In the MFB, the non-linear algebraic system (12) has been rewritten as

$$-\omega^{*2} \bar{a}_s \bar{m}^*_{sr} + \bar{a}_s \bar{k}^*_{sr} + \bar{a}_s \bar{a}_u \bar{a}_v \bar{b}^*_{suvr} = 0, \quad r = 1 - n \tag{15}$$

in which $\bar{k}^*_{sr}$, $\bar{m}^*_{sr}$ and $\bar{b}^*_{suvr}$ are the FCRP modal parameters calculated in the MFB. The analytical expressions, and numerical values of these parameters for FCRP with $\alpha = 0.6$, and $\alpha = 1$, are given in Appendix A, with the eigenvalues and eigenvectors obtained from the linear solution. Assuming in the MFB a contribution vector $\{\bar{A}\}^T = \{\bar{a}_1 \bar{\varepsilon}_2 ... \bar{\varepsilon}_n\}$, and applying an analysis similar to that made above in the BFB, leads to

$$\bar{\varepsilon}_r = -\frac{\frac{3}{2} \bar{a}_1^3 \bar{b}^*_{111r}}{\bar{k}^*_{rr} - \omega^{*2} \bar{m}^*_{rr}} \quad (r = 2, 3, ..., 9). \tag{16}$$

These simple expressions have led, in the case of FCRP with an aspect ratio $\alpha = 0.6$, to accurate values for the basic function contributions, compared with the iterative numerical solution of the non-linear algebraic system, for maximum plate vibration amplitudes, reached at the plate centre $(x^*, y^*) = (0.5, 0.5)$, up to about 0.6 times the plate thickness, for the first non-linear FCRP mode shape. It was shown in Ref. [12] that, for amplitudes of vibration up to once the plate thickness, the error induced by this first formulation does not exceed 0.066% for the non-linear frequency, and 5.62% for the associated non-linear bending stress obtained at point (0.25,0), chosen in the region in which the maximum value of σ^*_{yb} is reached.

2.4. Exact solution, based on use of elliptic functions, for solution of the one-dimensional Duffing equation, obtained by application of the single-mode approach to the multi-mode model for non-linear free vibrations of FCRP

2.4.1. Introduction

In this subsection, non-linear free vibration of rectangular plates with various boundary conditions is considered. The amplitude dependence of the non-linear frequency obtained via exact elliptical solution of Eq. (11), based on the single-mode approach, is compared with other previously published, approximate solutions. It should be noted that such an exact analytical solution of the Duffing equation is known and has been mentioned for example in Ref. [9] (and in Refs. [9,29] of Ref. [9]). The purpose of the present subsection is determination of the specific solutions for FCRP, with the corresponding numerical values of the equation parameters, and use of the power expansion of the exact solution obtained in order to determine acceptable approximate expressions for non-linear frequencies, valid for a large interval of vibrations amplitudes, exceeding the radius of convergence of the analytical series, based on the Padé approximants. It should also be noted here that another exact solution of the non-linear equation of motion, expressed in a manner that can be evaluated numerically to any desired degree of accuracy, has also been presented in Ref. [19], based on a procedure which eliminates the singularities in the expression of the non-linear frequency and yields a form which can be integrated numerically.

2.4.2. Exact solution based on use of elliptic functions

Applying the one mode assumption to Eq. (9) leads to

$$m_{11}^{*}\omega^{2}q_{1,\tau\tau}+\left(\frac{\omega}{\omega_{L}}\right)^{2}\left[q_{1}+\beta q_{1}^{3}\right]=0, \tag{17}$$

where $\beta=2b_{1111}^{*}/k_{11}^{*}$. The exact mathematical solution of Eq. (17) can be given in terms of the Jacobean elliptic function C_n [9]. The assumption that the solution $q_1(\tau)$ is periodic with a period of 2π gives the final form of this solution:

$$q_{1}(\tau)=a_{1}C_{n}(\gamma\tau,k), \tag{18}$$

$$\left(\frac{\omega}{\omega_{L}}\right)^{2}=\frac{\left(\frac{\pi^{2}}{4}\right)\left(1+\beta a_{1}^{2}\right)}{[K(k)]^{2}}, \tag{19}$$

$$K(k)=\int_{0}^{\pi/2}\frac{\mathrm{d}\theta}{\sqrt{1-k^{2}\sin^{2}\theta}}, \tag{20}$$

$$k^{2}=\frac{\beta a_{1}^{2}}{(2+2\beta a_{1}^{2})}, \tag{21}$$

$$\gamma=\left(\frac{\omega_{L}}{\omega}\right)\sqrt{1+\beta a_{1}^{2}} \tag{22}$$

in which k is the modulus of the elliptic function and γ may be taken as the "circular frequency". Using a perturbation method, as in Ref. [9], for small values of a_1, the modulus k is also small, $C_n(\gamma\tau, k)$ can be approximated by $\sin \omega t$.

Expanding the elliptic function $K(k)$ as a power series of a_1, Eq. (20) leads to

$$\left(\frac{\omega}{\omega_L}\right)^2 = 1 + \tfrac{3}{4}\beta a_1^2 - \tfrac{3}{128}\beta^2 a_1^4 + O(a_1^6). \tag{23}$$

Finally, the first approximation of the exact solution, obtained by truncating the above series at the second order, is given by

$$q_1(t) = a_1 \sin \omega t, \tag{24a}$$

$$\left(\frac{\omega}{\omega_L}\right)^2 = 1 + \tfrac{3}{4}\beta a_1^2. \tag{24b}$$

The results obtained by the exact solution, and by the first approximation of the exact solution at the second order, will be compared in Section 2.4.3 with those obtained by use of two Padé approximants.

2.4.3. Improvement of the solution, based on use of the Padé approximants

An extensive discussion has been made in Ref. [9] concerning the limitation in the choice of the polynomial approximation used in the power series expansion of the exact solution (20), given in Eq. (23), because of the divergence of the solution obtained outside the zone of convergence. It was demonstrated that increasing the order of the series does not increase the validity of the solution because of the divergence beyond the radius of convergence. It appeared also in this study that the second order approximated solution (24b) is the best one because it remains very close to the exact solution over a large range of vibration amplitudes. It has been also shown that use of the Padé approximant denoted as $P[M,N]$, which is defined as the quotient of two polynomials of degree M and N respectively, increases the range of validity of different approximation methods based on the perturbation method. A criterion which has worked well here is the choice of $P[M,N]$ such that $M-N=2$. So, two approximants have been used here, giving a good accuracy from comparison with the exact solution at large vibration amplitudes:

$$\left(\frac{\omega}{\omega_L}\right)^2 = P[4,2](a_1) = \frac{1}{32}\left(\frac{128 + 192\beta a_1^2 + 69\beta^2 a_1^4}{4 + 3\beta a_1^2}\right), \tag{25}$$

$$\left(\frac{\omega}{\omega_L}\right)^2 = P[6,4](a_1) = \frac{1}{4}\left(\frac{4096 + 9216\beta a_1^2 + 6748\beta^2 a_1^4 + 1605\beta^3 a_1^6}{1024 + 1536\beta a_1^2 + 559\beta^2 a_1^4}\right). \tag{26}$$

These relationships have been established in Ref. [9] for the beam case, but can also be used in the FCRP case at large vibrations amplitudes, since the latter case is also governed by the same equation, in which the value of the parameter $\beta = 2b^*_{1111}/k^*_{11}$ has to be calculated according to the theory developed for plates in the previous sections.

It can be seen in Table 1, that for non-dimensional amplitudes of vibrations up to $w^*_{max} = 2.5$, corresponding to $a_1 = 1$, the solutions obtained by the three approximations, i.e., Eqs. (24b), (25) and (26), are very close to those obtained by the exact solution. The differences between the exact

Table 1
Comparison of the frequency ratio ω/ω_L obtained by the exact elliptic solution with the improved approximate solutions obtained by using the Padé approximants for FCRP

a_1	ex-sol Eq. (19)	$P(4,2)$ Eq. (25)	$P(6,4)$ Eq. (26)	order 2 Eq. (24b)
0.200	1.06162341	1.06162352	1.06162341	1.06190703
0.300	1.13337139	1.13337313	1.13337139	1.13455045
0.400	1.22612026	1.22613022	1.22612029	1.22905906
0.500	1.33527261	1.33530509	1.33527280	1.34081725
0.600	1.45705459	1.45712992	1.45705521	1.46588502
0.700	1.58854813	1.58868850	1.58854965	1.60114651
0.800	1.72755253	1.72777837	1.72755551	1.74423183
0.900	1.87241967	1.87274782	1.87242468	1.89336803
1.000	2.02191259	2.02235594	2.02192017	2.04723315

solution and the approximations do not exceed 0.022% for $P(4,2)$, 0.00037% for $P(6,4)$, and 1.25% for the order 2.

3. Theoretical formulation for the geometrically NLSSPFR problem of FCRP excited harmonically by concentrated or distributed forces

3.1. Introduction

The purpose of Section 3 is the extension of the model presented above for non-linear free vibrations of FCRP, to the case of geometrically NLSSPFR of FCRP, excited harmonically by concentrated or distributed forces. Then, various degrees of approximation will be examined for the solution of the general model obtained, as discussed in Section 4.

3.2. Formulation of the problem of the NLSSPFR of FCRP in the BFB

Consider a FCRP excited by a concentrated harmonic force F^c applied at the point (x_0, y_0), or by a distributed harmonic uniform force F^d, distributed over the range $\bar{S}$ ($\bar{S}$ is the surface of the plate or a part of it). F^c and F^d may be written using the Dirac function δ as

$$F^c(x, y, t) = F^c\delta(x - x_0)\delta(y - y_0)\sin\,\omega t, \tag{27}$$

$$F^d(x, y, t) = F^d\,\sin\,\omega t \quad \text{if } (x, y) \in \bar{S}, \tag{28a}$$

$$F^d(x, y, t) = 0 \quad \text{if } (x, y) \notin \bar{S}. \tag{28b}$$

The corresponding generalized forces $F_i^c(t)$ and $F_i^d(t)$ in the BFB are given by

$$F_i^c(t) = F^c w_i(x_0, y_0)\,\sin\,\omega t = f_i^c\,\sin\,\omega t, \tag{29a}$$

$$F_i^d(t) = F^d\,\sin\,\omega t \int_{\bar{S}} w_i(x, y)\mathrm{d}x\mathrm{d}y = f_i^d\,\sin\,\omega t. \tag{29b}$$

The dimensionless generalized forces f_i^{*c} and f_i^{*d} corresponding, respectively, to the concentrated force F^c at point (x_0,y_0), or its non-dimensional equivalent (x_0^*, y_0^*), and to the uniformly distributed force F^d over the surface $\bar{S}$, or its non-dimensional equivalent $\bar{S}^*$, for a FCRP having the characteristics a, b, H and D, have been calculated in Appendix A. The expressions obtained are

$$f_i^{*c} = \frac{b^3 F^c}{aDH} w_i^*(x_0^*, y_0^*), \tag{30}$$

$$f_i^{*d} = \frac{b^4 F^d}{DH} \int\int_{s^*} w_i^*(x^*, y^*) \mathrm{d}x^* \mathrm{d}y^*. \tag{31}$$

A forcing vector $\{\mathbf{F}^*(t)\}$ is defined by: $\{\mathbf{F}_i^*(t)\} = \{\mathbf{f}_i^{*c}\} \sin \omega t$, or $\{\mathbf{F}_i^*(t)\} = \{\mathbf{f}_i^{*d}\} \sin \omega t$, depending on the type of excitation considered. Adding the forcing term $\{F^*(t)\}$ to the right hand side of Eq. (9) written in the BFB leads to

$$[\mathbf{M}^*]\{\mathbf{q}_{\tau\tau}\} + [\mathbf{K}^*]\{\mathbf{q}\} + 2[\mathbf{B}^*(\{\mathbf{q}\})]\{\mathbf{q}\} = \{\mathbf{F}^*(t)\}. \tag{32}$$

This equation appears as a generalization to the non-linear case of the classical forced response matrix equation, well known in linear modal analysis theory [20] as

$$[\mathbf{M}^*]\{\mathbf{q}_{\tau\tau}\} + [\mathbf{K}^*]\{\mathbf{q}\} = \{\mathbf{F}^*(t)\} \tag{33}$$

to which the correcting term $2[\mathbf{B}^*(\{\mathbf{q}\})]\{\mathbf{q}\}$, corresponding to the non-linear geometrical rigidity is added. If harmonic excitation is assumed, as in Eqs. (29a) and (29b), the linear system (33) leads to a harmonic solution, which may be expressed analytically in the MFB, in which the system is uncoupled. The response is obtained as a superposition of modal contributions, whose expressions are given in Section 4. In the non-linear case, previous experimental and theoretical works have shown that a harmonic distortion of the response occurs at large vibration amplitudes, which is accentuated in the clamps region, even when the excitation is harmonic. Since it was shown, via experimental measurements and a careful separation of harmonics, that the harmonic distortion was spatially distributed, the non-linear response may be written as [3]

$$W = \{\mathbf{A}_k\}^{\mathrm{T}} \{\mathbf{W}\} \sin k\omega t, \tag{34}$$

where $\{\mathbf{A}_k\}^{\mathrm{T}} = [a_1^k a_2^k ... a_n^k]$ is the matrix of coefficients corresponding to the kth harmonic, $\{\mathbf{W}\}^{\mathrm{T}} = [w_1 w_2 ..... w_n]$ is the basic spatial functions matrix, k is the number of harmonics taken into account, and the usual summation convention on the repeated index k is used . Examination of this effect would have exceeded the scope of the present work, which is restricted to the first harmonic distribution amplitude dependence, so that the response is written as

$$W(x, y) = a_i w_i(x, y) \sin \omega t. \tag{35}$$

The time-dependent contribution vector $\{\mathbf{q}\}^{\mathrm{T}} = [q_1 q_2 ... q_n]$ can therefore be replaced in Eq. (32) by $\{\mathbf{q}\} = \{\mathbf{A}\} \sin \omega t$, with $\{\mathbf{A}\}^{\mathrm{T}} = [a_1 a_2 ... a_n]$ representing the time-independent basic function contributions vector. This leads to

$$([\mathbf{K}^*] - \omega^2 [\mathbf{M}^*])\{\mathbf{A}\} \sin^2 \omega t + 2[\mathbf{B}^*(\mathbf{A})]\{\mathbf{A}\} \sin^3 \omega t = \{\mathbf{f}_i^*\} \sin \omega t \tag{36}$$

in which $\{\mathbf{f}_i^*\}$ equals $\{\mathbf{f}_i^{*c}\}$ or $\{\mathbf{f}_i^{*d}\}$, depending on the type of excitation under examination. Applying the harmonic balance method to Eq. (36) leads to

$$([\mathbf{K}^*] - \omega^2 [\mathbf{M}^*])\{\mathbf{A}\} + \tfrac{3}{2}[\mathbf{B}^*(\mathbf{A})]\{\mathbf{A}\} = \{\mathbf{f}_i^*\}. \tag{37}$$

This equation appears as a generalization to the non-linear case of the classical eigenvalue problem, well known in linear modal analysis theory, i.e.,

$$\left(\left[\mathbf{K}^*\right] - \omega^{*2}\left[\mathbf{M}^*\right]\right)\{\mathbf{A}\} = \left\{\mathbf{f}_i^*\right\} \tag{38}$$

to which the geometrically non-linear rigidity term $\frac{3}{2}\left[\mathbf{B}^*(\mathbf{A})\right]\{\mathbf{A}\}$ has been added. Eq. (37) can be written using the tensor notation as

$$a_i k_{ir}^* - \omega^{*2} a_i m_{ir}^* + \tfrac{3}{2} a_i a_j a_k b_{ijkr}^* = f_i^* \quad \mathrm{i} = 1...n. \tag{39}$$

The last non-linear algebraic system, corresponding to the NLSSPFR of FCRP, is similar to that obtained for the free vibration case, i.e., Eq. (12), with three differences. (1) In the free case, i varies from 2 to n, and the first equation is omitted, because the first contribution a_1 was assigned, as explained in the discussion following Eq. (13). (2) All of the n equations have a right-hand side representing the generalised forcing term f_i^*. (3) The frequency parameter ω^* does not represent, as in Eq. (12), the non-linear resonant frequency associated with a given amplitude of vibration, but represents the excitation frequency, which varies in the range chosen for performing the excitation tests, or for examining theoretically the NLSSPFR. Also, it may be worth noting here, that system (39) is formally identical to that obtained in Ref. [9], and used to obtain the NLSSPFR of various beams [9,10].

3.3. Formulation in the MFB

As stated in the above section, the explicit analytical solution of the linear system (33) can be obtained only if the problem is uncoupled via use of the normal modes basis of the FCRP considered, i.e., the MFB. Also, it was shown in Ref. [12] that the accurate explicit analytical solution corresponding to the non-linear free vibration case of FCRP can be obtained only in the MFB. So, the NLSSPFR problem will also be formulated here in this appropriate basis, using the notation of Ref. [12]. Consider now the NLSSPFR problem of FCRP, formulated in the BFB by the non-linear system (32). In the MFB, the generalized forces $\bar{F}_i^c(t)$ and $\bar{F}_i^d(t)$ are given by

$$\bar{F}_i^c(t) = F^c \phi_i^*(x_0, y_0) \sin \omega t = \bar{f}_i^c \sin \omega t, \tag{40a}$$

$$\bar{F}_i^d(t) = F^d \sin \omega t \int_{\bar{S}} \phi_i(x, y)\mathrm{d}x\mathrm{d}y = \bar{f}_i^d \sin \omega t \tag{40b}$$

in which the ϕ_i's are the elements of the MFB, defined in Ref. [12]. The dimensionless generalized forces $\bar{f}_i^{*c}$ and $\bar{f}_i^{*d}$ corresponding to a concentrated harmonic force F^c, applied at $\left(x_0^*, y_0^*\right)$, and a distributed harmonic force F^d, uniformly applied over the surface $\bar{S}$, for a FCRP having the characteristics a, b, H and D are given by

$$\bar{f}_i^{*c} = \frac{b^3 F^c}{aDH} \phi_i^*(x_0^*, y_0^*), \tag{41}$$

$$\bar{f}_i^{*d} = \frac{b^4 F^d}{DH} \int \int_{\bar{S}^*} \phi_i^*(x^*, y^*)\mathrm{d}x^*\mathrm{d}y^*. \tag{42}$$

Rewriting Eq. (32) in the MFB gives

$$\left[\bar{\mathbf{M}}^*\right]\{\bar{\mathbf{q}}_{\tau\tau}\} + \left[\bar{\mathbf{K}}^*\right]\{\bar{\mathbf{q}}\} + 2\left[\bar{\mathbf{B}}^*(\{\bar{\mathbf{q}}\})\right]\{\bar{\mathbf{q}}\} = \left\{\bar{\mathbf{F}}^*(t)\right\} \tag{43}$$

in which $[\bar{\mathbf{M}}^*]$ and $[\bar{\mathbf{K}}^*]$ are the diagonal mass and rigidity matrices calculated in the MFB, and $[\bar{\mathbf{B}}^*]$ is the non-linear rigidity tensor, calculated also in the MFB. Eq. (43) appears as a generalization to the non-linear case of the classical linear forced response problem, well known in modal analysis theory [20], i.e.,

$$\left[\bar{\mathbf{M}}^*\right]\{\bar{\mathbf{q}}_{\tau\tau}\} + \left[\bar{\mathbf{K}}^*\right]\{\bar{\mathbf{q}}\} = \left\{\bar{\mathbf{F}}^*(t)\right\} \tag{44}$$

to which the correcting term $2[\bar{\mathbf{B}}^*(\{\bar{\mathbf{q}}^*\})]\{\bar{\mathbf{q}}^*\}$, corresponding to the non-linear geometrical rigidity, is added. Assuming, as in the previous section, that harmonic motion takes place, leads to

$$\bar{q}_i(t) = \bar{a}_i \sin \omega t \tag{45}$$

for $i = 1$–n. Substituting Eq. (45) into Eq. (43), and applying the harmonic balance method, gives

$$\left(\left[\bar{\mathbf{K}}^*\right] - \omega^{*2}\left[\bar{\mathbf{M}}^*\right]\right)\{\bar{\mathbf{A}}\} + \tfrac{3}{2}\left[\bar{\mathbf{B}}^*(\{\bar{\mathbf{a}}\})\right]\{\bar{\mathbf{a}}\} = \left\{\bar{\mathbf{f}}_i^*\right\}. \tag{46}$$

This equation is the extension to the non-linear case of the classical linear eigenvalue problem, obtained in linear modal analysis theory [20], i.e.,

$$\left(\left[\bar{\mathbf{K}}^*\right] - \omega^{*2}\left[\bar{\mathbf{M}}^*\right]\right)\{\bar{\mathbf{A}}\} = \left\{\bar{\mathbf{f}}_i^*\right\} \tag{47}$$

to which the correcting term $\frac{3}{2}\left[\mathbf{B}^*(\mathbf{A})\right]\{\mathbf{A}\}$, corresponding to the non-linear geometrical rigidity is added. The linear response obtained from solution of Eq. (47) is given by a function $W^*_{\omega^*}(x^*, y^*, t)$ obtained as a superposition of modal contributions:

$$W^*_{\omega^*}(x^*, y^*, t) = \sin \omega t \sum_i \bar{a}_i \phi_i^*(x^*, y^*) = \sum_i \frac{\bar{f}_i^*}{(\bar{k}_{ii}^* - \omega^{*2}\bar{m}_{ii}^*)} \phi_i^*(x^*, y^*) \sin \omega t. \tag{48}$$

The linear frequency response function (48) can be rewritten using the notation corresponding to the MFB, and the repeated indices summation convention as

$$W^*_{\omega^*}(x^*, y^*) = \bar{a}_i \phi_i^*(x^*, y^*) \sin \omega t. \tag{49}$$

Returning now to the main purpose, i.e., the NLSSPFR of FCRP, system (46) may be written using the tensor notation as

$$-\omega^{*2}\, \bar{a}_s \bar{m}_{sr}^* + \bar{a}_s \bar{k}_{sr}^* + \tfrac{3}{2}\bar{a}_s \bar{a}_u \bar{a}_v \bar{b}_{suvr}^* = \bar{f}_r^*, \quad r = 1-n \tag{50}$$

which is a system of n coupled non-linear algebraic equations, whose solution should lead to a multi-dimensional non-linear frequency response function, describing the behaviour of FCRP subjected to high levels of harmonic excitation, so that the deflection shapes become amplitude dependent, and exhibit in the neighbourhood of each resonant frequency multi-valued regions in which the jump phenomenon may occur.

4. Solutions of the coupled non-linear differential equations for the NLSSPFR of FCRP

4.1. Discussion of the solutions procedures

Before presenting in the next subsections the methods of solution proposed in the present paper for the multi-dimensional Duffing equation (43) describing the NLSSPFR of FCRP, a discussion of many aspects of the various solution procedures which may be adopted for such a coupled non-linear problem is made here.

The modelling of very complicated problems, such as geometrically non-linear vibrations of FCRP considered here, for which no exact solution is known, even in the linear case, involves many choices based on the following observations:

(a) Due to the complexity of the real non-linear dynamic behaviour, and the variety of the phenomena involved (harmonic distortion, internal resonance, bifurcation points, non-linear coupling between modes, multiplicity of solutions, effect of damping, etc.), it is very difficult to develop a reasonable model including all of the known effects. So, a given model necessarily should be directed towards predicting specific effects, and hence, should be based on a decision to include or not each of the known physical aspects of the non-linear dynamic behaviour of the structure considered. Although this automatically limits the domain of validity of the model, it seems normal to do so in the modelling of very complex problems, because, as outlined in Ref. [21], each particular approach can only highlight one or a few facets of the problem, and is valid under specific conditions. Of course, it is always good to attempt and include the maximum number of effects in a unified model, when it is possible to do so, but this should not make the formulation too complex, and understandable only by a small number of experts. Also, the computing time should not become too costly, as discussed below.

(b) One may be tempted to increase the numerical accuracy of the solution obtained, via an increase in the number of degrees of freedom of the system, an increase in the complexity of the formulation, and in the computing time. However, this does not seem to be always justified, since the various assumptions involved in the theoretical formulation, and the various approximations used in the solution process automatically limit the expected accuracy of the solutions. In such conditions, attempting too exact a numerical solution, i.e., solutions involving a large number of decimals, may be meaningless, and also often useless.

(c) A choice could be made between sacrificing, to a reasonable extent, the numerical accuracy of the solution, and hence reducing its domain of validity, but focusing on the elegance and simplicity of the description, or the rapidity of the solution. This strategy may be realistic in many cases, in view of the applications made of the model, and is, to a great extent, justified by the insight it gives into a given aspect of the physical behaviour, which is important from the conceptual point of view. Also, it generally induces great economy and facility in the solution process. In a paper entitled "Insight, not numbers" [22], it is stated that "The beauty and elegance of a modal representation is that it describes the dynamic properties of a structure in terms of simple oscillators and geometrically intuitive deformation patterns, and that only a limited number of modes are necessary to specify the dynamic behaviour in any given frequency band".

Due to the above remarks, many strategies for solving the non-linear system (32) will be considered below, responding to various choices among the points (a)–(c) presented above. Three approximate methods of solution of the non-linear algebraic system are proposed and compared with previous results. The first, based on the single-mode approach, assumes a significant contribution $\bar{a}_1$ of the first mode, and neglects completely the contributions $\bar{a}_r$ of the higher modes, for $r=2$—n. The second and third assume that the higher mode contributions are not equal to 0, but are small compared to the first contribution. This leads to explicit analytical expressions for the NLSSPFR of FCRP, or to numerical results obtained via solution of reduced linear systems of eight equations and eight unknowns, for each value of the level and the frequency of the excitation. The advantages and disadvantages of each of the above methods have been discussed in the general introduction of this paper. A numerical solution of the non-linear system (32), based on an iterative procedure, for various FCRP aspect ratios will be presented later.

4.2. Solutions based on the single-mode approach

4.2.1. Introduction

The single-mode assumption neglects all co-ordinates except a single "resonant" co-ordinate. Thus, it reduces the multi-degree-of-freedom system to a single-degree-of-freedom system. It has been shown in previous studies that such an assumption may not be very rigorous, with regard to some effects in non-linear vibration of structures, such as the increase of curvature near the clamps of a C–C beam [4], or the non-linear increase in curvatures and stresses in the clamps regions of FCRP, both homogeneous and composite [15–17]. However, the single mode approach has been very often used in the literature [23–29]. This is due to the great simplification it introduces in the theory on one hand, and on the other hand because the error it introduces in the estimation of the non-linear frequency remains very small for a large range of vibration amplitudes, as has been shown for example in Ref. [12].

4.2.2. Formulations in the BFB and the MFB

In this section, in which the single-mode approach is applied in the BFB, the NLSSPFR of the FCRP excited harmonically is assumed to involve only the first basic function w_{11}^*. The excitation frequency is chosen in the neighbourhood of the first resonant frequency. So, Eq. (32) reduces to

$$m_{11}^* q_{1,\tau\tau} + k_{11}^* q_1 + 2b_{1111}^* q_1^3 = f_1^* \sin \omega t \tag{51}$$

in which m_{11}^*, k_{11}^*, and b_{1111}^* are the mass, rigidity, and non-linearity terms corresponding to the first basic function, respectively, and f_1^* is the corresponding generalized force . Assuming a harmonic response $q_1 = a_1 \sin\omega t$, and applying the harmonic balance method leads to

$$(k_{11}^* - \omega^{*2} m_{11}^*) a_1 + \tfrac{3}{2} b_{1111}^* a_1^3 = f_1^*. \tag{52}$$

Introducing in Eq. (52) the linear frequency parameter $\omega_L^{*2} = k_{11}^*/m_{11}^*$ and rearranging leads to

$$\left(\frac{\omega^*}{\omega_L^*}\right)^2 = 1 + \tfrac{3}{2} b_{1111}^* \frac{a_1^2}{k_{11}^*} - \left(\frac{1}{k_{11}^*}\right)\frac{f_1^*}{a_1}. \tag{53}$$

This equation is similar to Eq. (32) obtained in Ref. [9] for the beam case. Results based on Eq. (53) are given in Section 4.4.2 for various FCRP aspects ratios and excitation levels, and compared with previously published data.

In order to improve the accuracy of the approximation based on the single-mode approach, as in the FCRP free vibration case, the single-mode approach can also be considered in the MFB, which reduces Eq. (43) to

$$\bar{m}^*_{11}\bar{q}_{1,\tau\tau} + \bar{k}^*_{11}\bar{q}_1 + 2\bar{b}^*_{1111}\bar{q}_1^3 = \bar{f}_1^* \sin \omega t \tag{54}$$

in which $\bar{m}^*_{11}$, $\bar{k}^*_{11}$, and $\bar{b}^*_{1111}$ are the mass, rigidity, and non-linearity terms corresponding to the FCRP first linear mode shape, respectively, and $\bar{f}^*_1$ is the corresponding generalized force. Assuming a harmonic response $\bar{q}_1 = \bar{a}_1 \sin \omega t$ and applying the harmonic balance method leads, in a manner similar to that developed in the above paragraph, to

$$\left(\frac{\omega^*}{\omega^*_L}\right)^2 = 1 + \tfrac{3}{2}\bar{b}^*_{1111}\frac{\bar{a}_1^2}{\bar{k}^*_{11}} - \left(\frac{1}{\bar{k}^*_{11}}\right)\frac{\bar{f}^*_1}{\bar{a}_1}. \tag{55}$$

This equation is formally identical to Eq. (53), in which the parameters calculated in the BFB are replaced by those calculated in the MFB. Numerical results based on Eq. (53) and (55) are discussed in Section 4.4.2.

4.3. Simplified theory for solution of the multi-mode model corresponding to the NLSSPFR of FCRP

In the above section, solutions of the multi-mode model (39) and (50), based on the single-mode approach, have been presented and compared with other results available in the literature. Although it was shown that such an approach, in addition to the advantage of its great simplicity, may lead to good results for reasonable ranges of excitation levels and vibration amplitudes, it cannot be applied to high excitation levels, for which the contributions of the higher basic functions to the response become very important.

The improved version of the semi-analytical model applied in Ref. [11] to the non-linear forced response of beams, has been extended in the present work to the case of FCRP. It made it possible to obtain analytically a more accurate estimation of the FCRP non-linear frequency response functions, via concentrated or distributed harmonic excitation forces. These functions involve the contributions of the higher basic functions and make it possible to take into account the amplitude dependence of the deflection shapes induced by the geometrical non-linearity.

This approach assumes that the higher mode contributions (to the NLSSPFR of FCRP) are small compared to the first basic function contribution but are not completely negligible as in the single-mode approach. This leads to the following analysis

Consider the non-linear system (50) and apply the first formulation. It consists of neglecting in the expression $\bar{a}_s\bar{a}_u\bar{a}_v\bar{b}^*_{suvr}$ of Eq. (50), which involves summation for the repeated indices s, u, v over the range $\{1, 2, \ldots, n\}$, both first and second order terms with respect to $\bar{\varepsilon}_i$, i.e. terms of the type $\bar{a}_1^2\bar{\varepsilon}_v\bar{b}^*_{11vr}$ or of the type $\bar{a}_1\bar{\varepsilon}_u\bar{\varepsilon}_v\bar{b}^*_{1uvr}$. The only remaining term in the expression $\bar{a}_s\bar{a}_u\bar{a}_v\bar{b}^*_{suvr}$ of Eq. (50) is $\bar{a}_1^3\bar{b}^*_{111r}$. Eq. (50) becomes

$$(\bar{k}^*_{rr} - \omega^{*2}\bar{m}^*_{rr})\bar{a}_r + \tfrac{3}{2}\bar{a}_1^3\bar{b}^*_{r111} = \bar{f}_r^* \quad \text{for} \quad (r = 2, \ldots, n). \tag{56}$$

This system makes it possible one to obtain explicitly the modal contributions $\bar{a}_2, ..., \bar{a}_n$ corresponding to a given value of the contribution $\bar{a}_1$ as follows:

$$\bar{a}_r = \frac{\bar{f}_r^* - \frac{3}{2}\bar{a}_1^3 \bar{b}_{r111}^*}{\bar{k}_{rr}^* - \omega^{*2}\bar{m}_{rr}^*} \quad (r = 2, ..., n). \tag{57}$$

The first harmonic component of the NLSSPFR function $W_{\omega^*}^*(x^*, y^*, t)$ is then given by

$$W_{\omega^*}^*(x^*, y^*, t) = \left[\frac{\bar{f}_1^* - \frac{3}{2}\bar{a}_1^3 \bar{b}_{1111}^*}{(\bar{k}_{11}^* - \omega^{*2}\bar{m}_{11}^*)} \phi_1^*(x^*, y^*) + \frac{\bar{f}_2^* - \frac{3}{2}\bar{a}_1^3 \bar{b}_{2111}^*}{(\bar{k}_{22}^* - \omega^{*2}\bar{m}_{22}^*)} \phi_2^*(x^*, y^*) + \cdots + \frac{\bar{f}_9^* - \frac{3}{2}\bar{a}_1^3 \bar{b}_{9111}^*}{(\bar{k}_{99}^* - \omega^{*2}\bar{m}_{99}^*)} \phi_9^*(x^*, y^*) \right] \sin \omega t. \tag{58}$$

Eq. (58) is an extension to the non-linear case of Eq. (48) obtained in linear modal analysis, in which the FCRP total response $W_{\omega^*}^*(x^*, y^*, t)$ appears as the sum of the linear response $W_{\omega^* l}^*(x^*, y^*, t)$ given by Eq. (48) and a non-linear term $W_{\omega^* nl}^*(x^*, y^*, t)$ given by

$$W_{\omega^* nl}^*(x^*, y^*, t) = -\frac{3}{2}\bar{a}_1^3 \left[\frac{\bar{b}_{1111}^*}{(\bar{k}_{11}^* - \omega^{*2}\bar{m}_{11}^*)} \phi_1^*(x^*, y^*) + \frac{\bar{b}_{2111}^*}{(\bar{k}_{22}^* - \omega^{*2}\bar{m}_{22}^*)} \phi_2^*(x^*, y^*) + ... + \frac{\bar{b}_{9111}^*}{(\bar{k}_{99}^* - \omega^{*2}\bar{m}_{99}^*)} \phi_9^*(x^*, y^*) \right] \sin \omega t. \tag{59}$$

The cubic non-linear term $\bar{a}_1^3$ may be obtained for a given value of the excitation frequency parameter ω^*, and a given value of the excitation force parameter $\bar{f}_1^*$, via Eq. (55) based on the single-mode approach. It is interesting to notice here that Eqs. (57) and (58) are formally identical to Eqs. (64) and (65) obtained for the NLSSPFR of various beams in Ref. [11].

The simplified theory presented in this subsection focuses on non-linear vibrations of plates using a multi-mode approach and taking into account the coupling between the higher vibration modes. The solution obtained in Eq. (59) makes it possible to get directly the non-linear frequency response function in the neighbourhood of the first mode. This gives not only the displacement at the centre of the plate, as is usually the case, as a function of the non-linear frequency, but also the plate response spatial distribution on its whole area, for each level of excitation. The deformed deflection shapes, obtained by this approach, agree well with the experimental data carefully measured in Ref. [13], and permit the associated non-linear stress distribution, which may be of a crucial importance in the design process to be deduced easily.

4.4. Comparison of the solutions based on the single-mode approach, and the simplified multi-mode approach, for the NLSSPFR of FCRP, with previous results obtained by others methods

4.4.1. Analytical details

In order to make comparisons of our results with those previously published , the different choices of normalization have to be standardized as follows :

In Ref. [30], the deflection function $W(x, y, t)$ was written in the form $W(x, y, t) = HAq(t)\phi(x, y)$, where $q(t)$ and $\phi(x, y)$ are time and spatial functions, normalized in such a manner that $\phi_{\max} = q_{max} = 1$. According to these notations, the maximum vibration amplitude

$W_{\max} = HA$. In the present work, W_{max} is given in the BFB by $W_{max} = Ha_1 w_1^*(C)$, in which C denotes the plate centre. So, the non-dimensional amplitude of vibration A, defined in Ref. [30], is related to the parameters defined here by $A = a_1 w_1^*(C)$. Using this notation, Eq. (53) can be written as

$$\left(\frac{\omega^*}{\omega_L^*}\right)^2 = 1 + \frac{3}{2}\left(\frac{b_{1111}^*}{k_{11}^*}\right)\frac{A^2}{(w_1^*(C))^2} - \frac{w_1^*(C) f_1^*}{k_{11}^* A} \tag{60}$$

which leads to

$$\left(\frac{\omega^*}{\omega_L^*}\right)^2 = 1 + \frac{3}{2}\left(\frac{b_{1111}^*}{k_{11}^*}\right)\frac{A^2}{(w_1^*(C))^2} - \frac{F}{A}. \tag{61}$$

Using the expression for f_1^*, obtained from Eqs. (30) and (31), for $i=1$, leads to

$$F^d = \frac{b^3 F^d}{DH}\ \frac{1}{k_{11}^*} w_1^*(C) \int\int_{s^*} w_1^*(x^*, y^*)\mathrm{d}x^*\mathrm{d}y^*, \tag{62}$$

$$F^c = \frac{b^3 F^c}{aDH}\ \frac{1}{k_{11}^*} w_1^*(C) w_1^*(x_0^*, y_0^*) \tag{63}$$

corresponding to the cases of a distributed and a concentrated force, respectively. Similarly, in the MFB $A = \bar{a}_1 \phi_1^*(C)$, which leads, after substitution and rearrangement to

$$\left(\frac{\omega^*}{\omega_L^*}\right)^2 = 1 + \frac{3}{2}\left(\frac{\bar{b}_{1111}^*}{\bar{k}_{11}^*}\right)\frac{A^2}{(\phi_1^*(C))^2} - \frac{\bar{F}}{A}, \tag{64}$$

where $\bar{F}$ is defined in the case of a distributed and a concentrated force, respectively, by

$$\bar{F}^d = \frac{b^3 \bar{F}^d}{DH}\ \frac{1}{\bar{k}_{11}^*} \phi_1^*(C) \int\int_{\bar{s}^*} \phi_1^*(x^*, y^*)\mathrm{d}x^*\mathrm{d}y^*, \tag{65}$$

$$\bar{F}^c = \frac{b^3 \bar{F}^c}{aDH}\ \frac{1}{\bar{k}_{11}^*} \phi_1^*(C) \phi_i^*(x_0^*, y_0^*). \tag{66}$$

As shown in Appendix B, the non-dimensional parameter $P_0 = cF_0/\rho H^2 \omega^2$ used in Refs. [30,31], is related to the non-dimensional parameters defined here in the BFB and the MFB, respectively by

$$P_0 = w_1^*(C)\frac{f_1^*}{k_{11}^*} \quad \text{and} \quad P_0 = \phi_1^*(C)\frac{\bar{f}_1^*}{\bar{k}_{11}^*}. \tag{67, 68}$$

The above expressions will be used for comparison purposes in the next section.

4.4.2. Comparison of numerical results

In order to make comparisons with previously published results, only the values of the excitation forces found in the literature could be used. In Table 2 and Fig. 2, the values of the forced vibration frequency ratio for FCRP subjected to a harmonic distributed force $P_0 = 0.2$ ($F_d = 873.82\,\mathrm{N/m^2}$), obtained by (a) solving Eq. (61) corresponding to the single-mode model expressed in the BFB (rigidity k_{11}^* and non-linear rigidity b_{1111}^*), (b) solving Eq. (64) corresponding

Table 2
Forced vibration frequency ratio ω/ω_L for a fully clamped square plate subjected to harmonic distributed force $P_0 = 0.2$ ($P_d = 873.82\,\mathrm{N/m^2}$

$A = W_{max}/H$	Eq. (61)	Eq. (64)	Eq. (58)	Asympt. numer. method [32]	Simple elliptic response [30]	FEM + linearization [25]	Finite element 54 d.o.f [30]	HFEM $P_0 = 3, P_i = 6$ [31]	HFEM $P_0 = 4, P_i = 7$ [31]
+0.2	0.1475	0.1470	0.1375	0.2159977	0.1200	0.1002	0.1180	0.2442	0.2432
−0.2	1.4218	1.4211	1.4207	1.4329863	1.4195	1.4178	1.4195	1.4399	1.4275
+0.4	0.7661	0.7649	0.7585	0.7531451	0.7483		0.7459		
−0.4	1.2596	1.2588	1.2562	1.2505342	1.2490		1.2477		
+0.6	0.9285	0.9262	0.9142	0.8948691	0.8951	0.8700	0.8905	0.8962	0.8971
−0.6	1.2364	1.2346	1.2276	1.2092921	1.2117	1.1932	1.2083	1.2114	1.2120
+0.8	1.0476	1.0438	1.0238	0.9911671	0.9941		0.9863		
−0.8	1.2639	1.2608	1.2467	1.2148796	1.2203		1.2137		
+1	1.1588	1.1535	1.1226	1.0768604	1.0822	1.0251	1.0700	1.0800	1.0803
−1	1.3202	1.3155	1.2913	1.2457381	1.2540	1.2045	1.2429	1.2491	1.2475

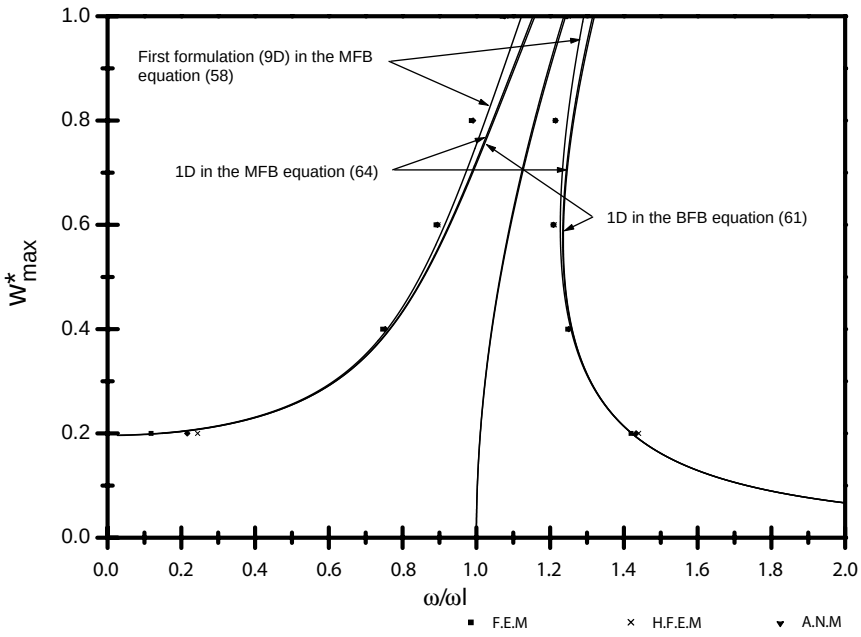

Fig. 2. Comparison of the forced response of a FCRP ($\alpha = 1$) subjected to harmonic distributed force $F_d = 0.2$ obtained with various present models. (a) Eq. (61), (b) Eq. 64, (c) Eq. (58), with previously published results, based on different other models. (■) F.E.M; (×) H. F.E.M.; (◆) A.N.M

to the single-mode model in the MFB (rigidity $\bar{k}^*_{11}$ and non-linear rigidity $\bar{b}^*_{1111}$), (c) using the simplified theory for solving the multi-mode model leading to Eq. (58), are compared with previously published results [25,30–32]. It can be concluded from Table 2 and Fig. 2 that the present results are very close to those based on other methods, for displacement amplitudes up to about 0.6 times the plate thickness. For higher amplitudes, situated between 0.6 and once the plate thickness, the results obtained from the multi-mode model are, as may be expected, closer to those obtained by the others numerical methods than those based on the single-mode approach. The average and standard deviation of all of the results available, obtained by various methods, are listed in Table 3. In Tables 4a and b, the percentage errors between the averages obtained in Table 3, and the values obtained by the single-mode approach, i.e., Eq. (64), and the simplified multi-mode approach, i.e., Eq. (58), are listed. It can be noted that these errors do not exceed 5% in all cases. For small amplitudes, i.e., amplitude less than 0.6 times the plate thickness, the errors induced by the two methods are comparable. For relatively high amplitudes, the error induced by the single-mode approach slightly exceeds that induced by the simplified multi-mode approach.

To evaluate the effect of the plate ratio aspect, the values of the forced vibration frequency ratio ω/ω_L of FCRP, with different aspect ratios, calculated from Eq. (61), are presented in Table 5. It can be seen that these values are very close to each other for this excitation level, but a trend of increase of the aspect ratio ω/ω_L may be noted when the aspect ratio decreases.

Forced responses of a fully clamped square plate, subjected to different distributed harmonic forces, are shown in Fig. 3. It can be seen from these curves that the single-mode model can be

Table 3
Average and standard deviation of the results given in Table 2 based on different approaches

W_{max}/H	Average	Standard deviation
0.2	1.6373E−01	5.5671E−02
−0.2	1.4245E+00	7.4695E−03
0.4	7.5614E−01	8.4475E−03
−0.4	1.2536E+00	5.1992E−03
0.6	9.0141E−01	1.8527E−02
−0.6	1.2161E+00	1.4038E−02
0.8	1.0145E+00	2.7555E−02
−0.8	1.2367E+00	2.3215E−02
1	1.0944E+00	4.2860E−02
−1	1.2634E+00	3.7858E−02

Table 4
Comparison between the average obtained in Table 3, and the results based on (a) single-mode approach, i.e., Eq. (64); (b) simplified multi-mode approach, i.e., Eq. (58)

W_{max}/H	Results based on the single mode approach	Average	Percentage error between the average and the single-mode approach
(a)			
0.2	0.147	1.6373E−01	1.18%
−0.2	1.4211	1.4245E+00	0.24%
0.4	0.7649	7.5614E−01	0.62%
−0.4	1.2588	1.2536E+00	0.36%
0.6	0.9262	9.0141E−01	1.75%
−0.6	1.2346	1.2161E+00	1.31%
0.8	1.0438	1.0145E+00	2.07%
−0.8	1.2608	1.2367E+00	1.70%
1	1.1535	1.0944E+00	4.18%
−1	1.3155	1.2634E+00	3.68%
W_{max}/H	Results based on the simplified multi-mode approach	Average obtained in Table 3	Percentage error between the average and the simplified multi-mode approach
(b)			
0.2	0.1375	1.6373E−01	1.85%
−0.2	1.4207	1.4245E+00	0.27%
0.4	0.7585	7.5614E−01	0.17%
−0.4	1.2562	1.2536E+00	0.18%
0.6	0.9142	9.0141E−01	0.90%
−0.6	1.2276	1.2161E+00	0.82%
0.8	1.0238	1.0145E+00	0.66%
−0.8	1.2467	1.2367E+00	0.71%
1	1.1226	1.0944E+00	2.00%
−1	1.2913	1.2634E+00	1.97%

Table 5
Forced vibration frequency ratio ω/ω_L for FCRP with different aspect ratios subjected to harmonic distributed force $P_0 = 0.2$ (Eq. (61))

$A = W_{max}/H$	$\alpha = 1$	$\alpha = 0.8$	$\alpha = 0.6$	$\alpha = 0.4$	$\alpha = 0.2$
+0.2	0.1475	0.1479	0.1492	0.1509	0.1523
−0.2	1.4218	1.4218	1.4220	1.4222	1.4223
+0.4	0.7660	0.7664	0.7673	0.7687	0.7698
−0.4	1.2596	1.2598	1.2605	1.2613	1.2619
+0.6	0.9285	0.9291	0.9308	0.9333	0.9353
−0.6	1.2364	1.2368	1.2382	1.2400	1.2415
+0.8	1.0476	1.0484	1.0512	1.0551	1.0583
−0.8	1.2639	1.2646	1.2669	1.2701	1.2728
+1	1.1588	1.1600	1.1640	1.1694	1.1739
−1	1.3201	1.3212	1.3247	1.3295	1.3335

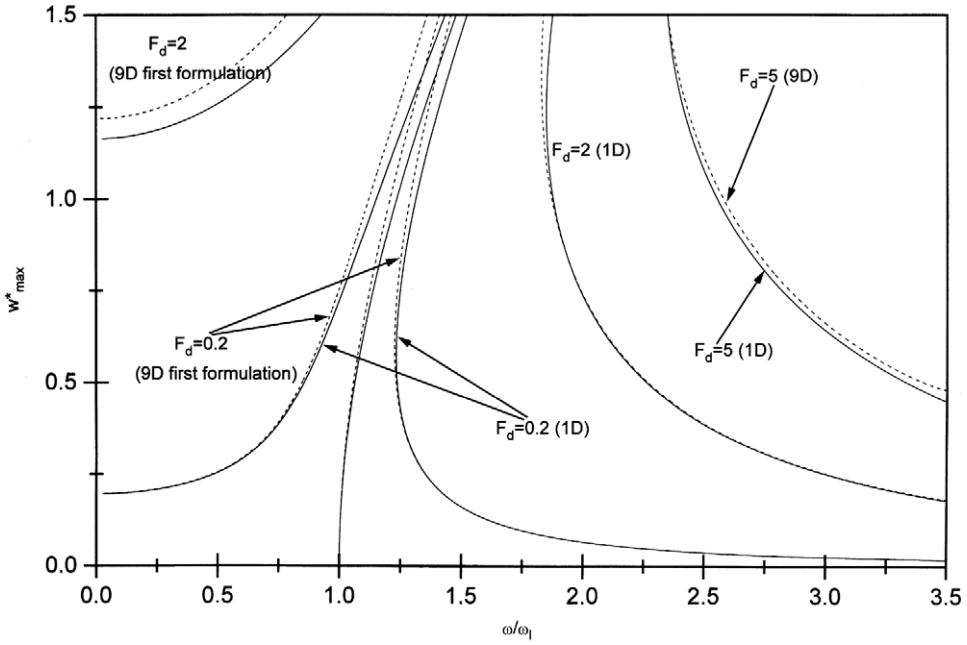

Fig. 3. Comparison of the forced response of a FCRP ($\alpha = 1$) subjected to harmonic distributed forces $F_d = 0.2$, $F_d = 2$, and $F_d = 5$, obtained with present model Eq. (58)

used for relatively small amplitudes of vibration, up to 0.5 times the plate thickness, for all of the levels of excitation considered.

In Table 6, the non-linear frequencies obtained by the single-mode model for different amplitudes of vibrations are compared with those obtained by other models [3,31,33,34], and with the multi-dimensional model. It can be concluded that for amplitudes of vibration up to 1* the

Table 6
Comparison of free vibration frequency ratios ω/ω_L for immovable fully clamped square isotropic plates

W_{max}/H	Ref. [33]	Ref. [34]	Ref. [31]	Ref. [31]	1-D present work	9-D Ref. [3]
0.2	1.0068	1.0095	1.0079		1.0072	1.0070
0.6	1.0600	1.0825	1.0632	1.0647	1.0632	1.0607
1	1.1599	1.2149	1.1670	1.1668	1.1670	1.1573

Table 7
Forced vibration frequency ratio ω/ω_L for a simply supported square plate subjected to harmonic distributed force $P_0 = 0.2$ ($P_d = 873.82\,N/m^2$

$A = W_{max}/H$	Eq. (61)	ANM [32]	Simple elliptic response [30]	FEM + linearization [25]	Finite element 54 d.o.f. [30]
+0.2	0.193985	0.2374288	0.1944	0.1622	0.1932
−0.2	1.426755	1.4333909	1.4281	1.4235	1.4274
+0.4	0.804378	0.8154793	0.8102		0.8052
−0.4	1.282975	1.2880868	1.2874		1.2839
+0.6	0.998339	1.0145738	1.0084	0.9506	0.9984
−0.6	1.289450	1.2990543	1.2983	1.2531	1.2898
+0.8	1.155506	1.1800401	1.1703		1.1528
−0.8	1.354659	1.3719442	1.3686		1.3524
+1	1.30945	1.3436439	1.3283	1.2075	1.3004
−1	1.454139	1.4809742	1.4276	1.3632	1.4460

plate thickness, the values of free vibration frequency ratios ω/ω_L, obtained by the single-mode model, or by the multi-mode model, are comparable with those obtained by the others models. This justifies use of the single-mode model for estimating in the free response case the non-linear resonance frequencies.

5. SSRP and CCCSSRP

Some results, based on the approach developed in above sections, are presented here, corresponding to SSRP and CCCSSRP. In Table 7 and Fig. 4, comparison is made between the results obtained here, based on the single-mode approach, for SSRP subjected to a harmonic distributed forces, with the results obtained in Ref. [25] via a finite element formulation. It can be seen that the single-mode model gives results which are very close to those previously published for amplitudes of vibration up to about 1* the plate thickness. Details concerning the simply supported plate parameters calculation are given in Appendix C.

Table 8 and Fig. 5 correspond to the single-mode approach applied to the case of CCCSSRP.

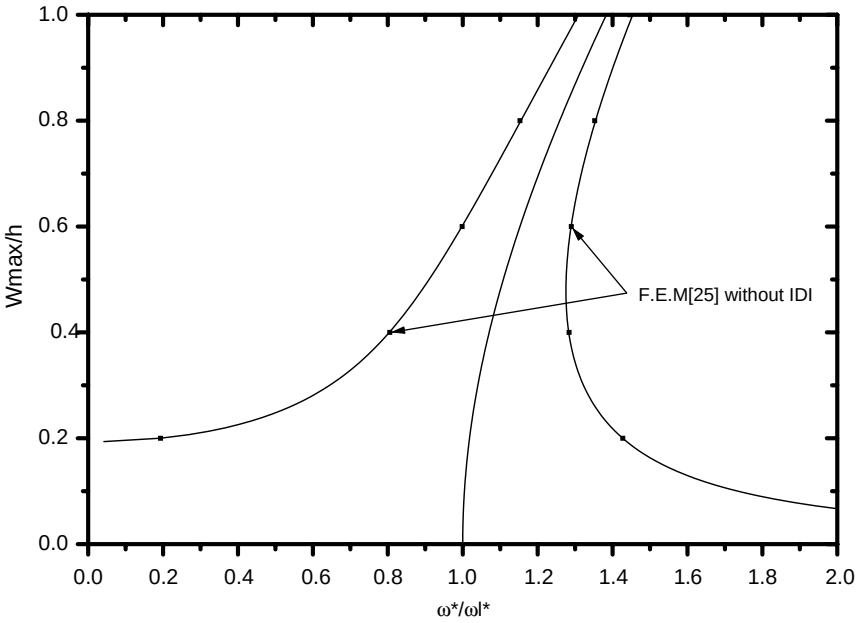

Fig. 4. Comparison of the forced response of a SSRP ($\alpha = 1$) subjected to harmonic distributed forces $F_d = 0.2$, obtained with present model Eq. (61), with a F.E. Model [25].

Table 8
Forced vibration frequency ratio ω/ω_L for a CCCSS square plate subjected to harmonic distributed force P_0

$A = W_{max}/H$	$P_0 = 0.1$	$P_0 = 0.2$
+0.2	0.7233	0.1528
−0.2	1.2341	1.4223
+0.4	0.9180	0.7699
−0.4	1.1587	1.2620
+0.6	1.0207	0.9356
−0.6	1.1727	1.2417
+0.8	1.1162	1.0587
−0.8	1.2230	1.2731
+1	1.2163	1.1744
−1	1.2959	1.3339

6. General conclusion

A semi-analytical approach to the non-linear dynamic response problem of beams has been developed, based on Lagrange's equations, and the harmonic balance method in Refs. [9,10]. This method has been successfully used here to determine the amplitude frequency dependence for the non-linear steady state periodic forced vibrations of FCRP. The dynamic problem is reduced to a set of non-linear algebraic equations depending on the classical rigidity and mass tensors, and a

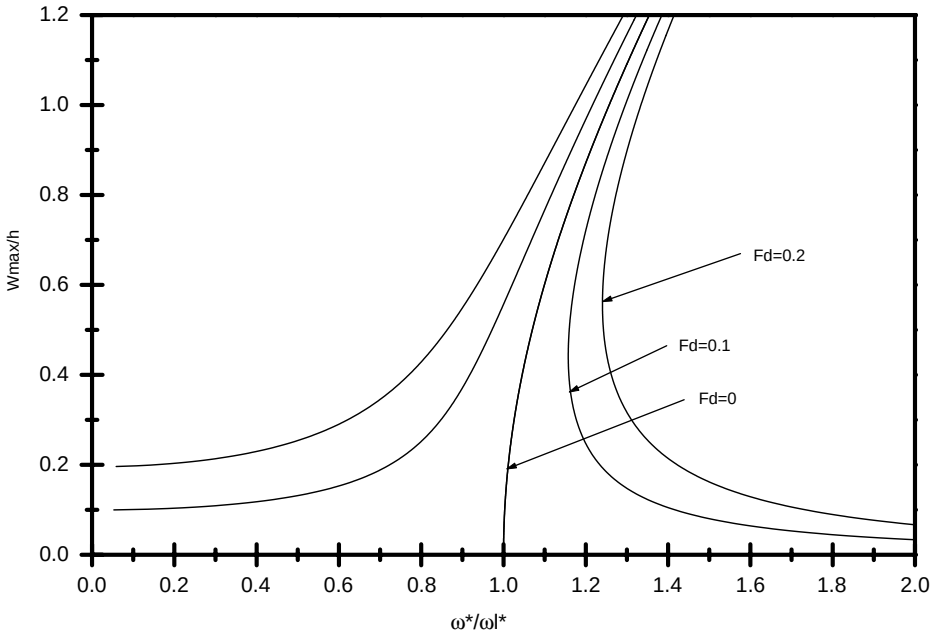

Fig. 5. Forced response of a CCCSSRP ($\alpha = 1$) subjected to harmonic distributed force F_d obtained with present model (Eq. (61)).

fourth order tensor due to the non-linearity. The single-mode analysis is presented here for the free and forced cases, leading to results which are in good agreement with those published previously.

An approach similar to that used in Refs. [11,12], for solving the multi-dimensional Duffing equation, for the non-linear free and NLSSPFR vibrations of beams, and the non-linear free vibrations of FCRP has been applied here to the NLSSPFR of FCRP. It has enabled explicit determination of the non-linear multi-mode steady state periodic forced response, for relatively small but finite vibration amplitudes, up to 0.8 times the plate thickness. The form of the explicit solution appears as a generalization to the non-linear case of the classical linear forced modal response. This may appear as one more step towards the development of the "non-linear modal analysis theory" mentioned in Refs. [11,12]. The single-mode model may be used to describe the dynamic problem, for vibration amplitudes up to 0.6 times the plate thickness, for the NLSSPFR of FCRP, and up to once the plate thickness for the NLSSPFR of SSRP. For higher amplitudes of vibrations, better results have been obtained by using a simplified multi-mode model for the steady state periodic forced response.

In addition to a better estimate of the non-linear frequency response function for a given level of excitation, the multi-mode simplified model makes it possible to obtain directly the amplitude-dependent deflection shapes of the rectangular plates at large vibration amplitudes, which is one of the most important features of the NLSSPFR of such structures at large vibration amplitudes, due to its important effect on curvatures and non-linear stresses.

Appendix A. Tensors definitions

$$m_{ij} = \rho H \int_S w_i(x,y) w_j(x,y)\, \mathrm{d}x\, \mathrm{d}y, \tag{A.1}$$

$$k_{ij} = \int_S D\left(\frac{\partial^2 w_i}{\partial x^2} + \frac{\partial^2 w_i}{\partial y^2}\right)\left(\frac{\partial^2 w_j}{\partial x^2} + \frac{\partial^2 w_j}{\partial y^2}\right)\mathrm{d}x\mathrm{d}y \tag{A.2}$$

$$b_{ijkl} = \frac{3D}{H^2}\int_S \left(\left(\frac{\partial \mathrm{w}_i}{\partial x}\right)\left(\frac{\partial \mathrm{w}_j}{\partial x}\right) + \left(\frac{\partial \mathrm{w}_i}{\partial y}\right)\left(\frac{\partial \mathrm{w}_j}{\partial y}\right)\right)\left(\left(\frac{\partial \mathrm{w}_k}{\partial x}\right)\left(\frac{\partial \mathrm{w}_l}{\partial x}\right) + \left(\frac{\partial \mathrm{w}_k}{\partial y}\right)\left(\frac{\partial \mathrm{w}_l}{\partial y}\right)\right)\mathrm{d}x\mathrm{d}y \tag{A.3}$$

$$w_i(x,y) = H w_i^*\left(\frac{x}{a}, \frac{y}{b}\right) = H w_i^*(x^*, y^*) \tag{A.4}$$

$$\frac{\omega^2}{\omega^{*2}} = \frac{D}{\rho H b^4}, \tag{A.5}$$

$$\frac{k_{ij}}{k_{ij}^*} = \frac{DaH^2}{b^3}, \tag{A.6}$$

$$\frac{m_{ij}}{m_{ij}^*} = \rho H^3 ab, \tag{A.7}$$

$$\frac{b_{ijkl}}{b_{ijkl}^*} = \frac{DaH^2}{b^3}. \tag{A.8}$$

A.1. Linear and non-linear modal parameters for the FCRP first non-linear mode shape (aspect ratio α=0.6)

(1) *Values of non-linear FCRP modal parameters: $\bar{b}_{i111}^*$ for the first non-linear FCRP mode shape*

$\bar{b}_{1111}^* = 1461.2099$ (MFB), $b_{1111}^* = 1586.7826$ (BFB),

$\bar{b}_{2111}^* = 609.1280$

$\bar{b}_{3111}^* = 178.0239$

$\bar{b}_{4111}^* = 964.3785$

$\bar{b}_{5111}^* = -47.9024$

$\bar{b}_{6111}^* = 202.5182$

$\bar{b}_{7111}^* = -2298.7265$

$\bar{b}_{8111}^* = 1164.5572$

$\bar{b}_{9111}^* = -198.9794$

(2) *Rigidity matrix for the first non-linear mode shape of FCRP with an aspect ratio α=0.6 expressed in the BFB*

$$\left[\mathbf{k}_{ij}^{*}\right]=\begin{bmatrix}
674.4143 & -86.1874 & -67.4566 & -86.1860 & 68.1604 & 53.3234 & -67.4299 & 53.3234 & 41.7161\\
-86.1874 & 15\,558.7014 & -215.8281 & 68.1604 & -692.9366 & 170.3977 & 53.3234 & -542.1252 & 133.3061\\
-67.4565 & -215.8281 & 91\,540.9905 & 53.3234 & 170.3977 & -1850.0956 & 41.7161 & 133.3061 & -1447.5055\\
-86.1860 & 68.1604 & 53.3234 & 3271.1858 & -692.9313 & -542.1285 & -215.5138 & 170.3977 & 133.3061\\
68.1604 & -692.9366 & 170.3977 & -692.9313 & 23\,556.5089 & -1732.6789 & 170.3977 & -1732.5269 & 425.9869\\
53.3234 & 170.3977 & -1850.0956 & -542.1285 & -1732.6789 & 109\,839.1056 & 133.3061 & 425.9869 & -4626.2467\\
-67.4299 & 53.3234 & 41.7161 & -215.5138 & 170.3977 & 133.3061 & 14\,391.9895 & -1850.0548 & -1447.3859\\
53.3234 & -542.1252 & 133.3061 & 170.3977 & -1732.5269 & 425.9869 & -1850.0548 & 44\,977.6201 & -4625.5414\\
41.7161 & 133.3061 & -1447.5055 & 133.3061 & 425.9869 & -4626.2467 & -1447.3859 & -4625.5414 & 15\,0903.9226
\end{bmatrix}.$$

(3) *First nine SSFCRP linear mode shapes (α=0.6)*

$$\boldsymbol{\phi}_1^{*}=\begin{bmatrix}0.9994\\0.0055\\0.0007\\0.0329\\-0.0020\\-0.0004\\0.0052\\-0.0012\\-0.0003\end{bmatrix},\quad \boldsymbol{\phi}_2^{*}=\begin{bmatrix}0.0329\\0.0041\\0.0006\\-0.9987\\-0.0342\\-0.0056\\-0.0181\\0.0020\\0.0007\end{bmatrix},\quad \boldsymbol{\phi}_3^{*}=\begin{bmatrix}0.0045\\0.0217\\0.0005\\0.0178\\0.0106\\0.0013\\-0.9976\\-0.0611\\-0.0127\end{bmatrix},\quad \boldsymbol{\phi}_4^{*}=\begin{bmatrix}0.0054\\-0.9954\\-0.0026\\-0.0005\\-0.0903\\0.0002\\-0.0211\\-0.0249\\0.0002\end{bmatrix},\quad \boldsymbol{\phi}_5^{*}=\begin{bmatrix}0.0037\\-0.0920\\-0.0024\\-0.0343\\0.9919\\0.0195\\0.0032\\0.0779\\0.0004\end{bmatrix},$$

$$\boldsymbol{\phi}_6^{*}=\begin{bmatrix}0.0012\\-0.0164\\-0.0015\\0.0059\\-0.0791\\-0.0054\\-0.0625\\0.9938\\0.0427\end{bmatrix},\quad \boldsymbol{\phi}_7^{*}=\begin{bmatrix}-0.0007\\-0.0025\\0.9937\\-0.0000\\-0.0000\\0.1073\\0.0001\\0.0006\\0.0325\end{bmatrix},\quad \boldsymbol{\phi}_8^{*}=\begin{bmatrix}0.0006\\0.0023\\-0.1102\\-0.0048\\-0.0196\\0.9879\\-0.0003\\-0.0009\\0.1070\end{bmatrix},\quad \boldsymbol{\phi}_9^{*}=\begin{bmatrix}0.0002\\0.0010\\-0.0206\\0.0012\\0.0053\\-0.1097\\-0.0100\\-0.0435\\0.9927\end{bmatrix}.$$

The above vector components are given in the BFB $=\{w_{11}^{*}, w_{13}^{*}, w_{15}^{*}, w_{31}^{*}, w_{33}^{*}, w_{35}^{*}, w_{51}^{*}, w_{53}^{*}, w_{55}^{*}\}$.

(4) *Diagonal rigidity matrix for the first non-linear mode shape of FCRP with an aspect ratio α=0.6 expressed in MFB*

$$\left[\bar{\mathbf{k}}^*_{ij}\right] = \begin{bmatrix} 670.4738 & & & & & & & & \\ & 3242.5882 & & & & & & & \\ & & 14\,261.2275 & & & & & & \\ & & & 15\,483.2756 & & & & & \\ & & & & 23\,475.3007 & & & & \\ & & & & & 45\,040.8070 & & & \\ & & & & & & 91\,294.6209 & & \\ & & & & & & & 109\,581.9417 & \\ & & & & & & & & 151\,664.2037 \end{bmatrix}.$$

A.2. Linear and non-linear modal parameters for the FCRP first non-linear mode shape aspect ratio α=1

(1) *Values of non-linear FCRP modal parameters: $\bar{b}^*_{i111}$ for the first non-linear FCRP mode shape α=1*

$$\begin{aligned} &\bar{b}^*_{1111} = 2782.9122\ (\text{MFB}),\ b^*_{1111} = 3001.8788\ (\text{BFB}),\\ &\bar{b}^*_{2111} = -6.1729\\ &\bar{b}^*_{3111} = -2177.8035\\ &\bar{b}^*_{4111} = -540.2969v\\ &\bar{b}^*_{5111} = -14.4508\\ &\bar{b}^*_{6111} = 3028.7144\\ &\bar{b}^*_{7111} = -71.5744\\ &\bar{b}^*_{8111} = 2037.8700\\ &\bar{b}^*_{9111} = 505.4647. \end{aligned}$$

(2) *Rigidity matrix for the first non-linear mode shape of FCRP with an aspect ratio α=1 expressed in the BFB*

$$\left[\mathbf{k}^*_{ij}\right] = \begin{bmatrix} 1303.8427 & -239.4063 & -187.3238 & -239.4063 & 189.3345 & 148.1207 & -187.3238 & 148.1207 & 115.8782 \\ -239.4063 & 17\,552.0347 & -598.8730 & 189.3345 & -1924.8110 & 473.3270 & 148.1207 & -1505.8742 & 370.2947 \\ -187.3238 & -598.8730 & 96\,135.4248 & 148.1207 & 473.3270 & -5139.0690 & 115.8782 & 370.2947 & -4020.5685 \\ -239.4063 & 189.3345 & 148.1207 & 17\,552.0347 & -1924.8110 & -1505.8742 & -598.8730 & 473.3270 & 370.2947 \\ 189.3345 & -1924.8110 & 473.3270 & -1924.8110 & 48\,803.1047 & -4812.4667 & 473.3270 & -4812.4667 & 1183.2970 \\ 148.1207 & 473.3270 & -5139.0690 & -1505.8742 & -4812.4667 & 155\,998.4600 & 370.2947 & 1183.2969 & -12\,848.8262 \\ -187.3238 & 148.1207 & 115.8782 & -598.8730 & 473.3270 & 370.2947 & 96\,135.4248 & -5139.0690 & -4020.5685 \\ 148.1207 & -1505.8742 & 370.2947 & 473.3270 & -4812.4667 & 1183.2969 & -5139.0690 & 155\,998.4600 & -12\,848.8262 \\ 115.8782 & 370.2947 & -4020.5685 & 370.2947 & 1183.2969 & -12\,848.8262 & -4020.5685 & -12\,848.8262 & 317\,759.6649 \end{bmatrix}.$$

(3) *First nine SSFCRP linear mode shapes (α=1)*

$$\boldsymbol{\phi}_1^* = \begin{bmatrix} -0.9998 \\ -0.0142 \\ -0.0020 \\ -0.0142 \\ 0.0031 \\ -0.0009 \\ -0.0020 \\ 0.0009 \\ 0.0004 \end{bmatrix}, \quad \boldsymbol{\phi}_2^* = \begin{bmatrix} 0.0000 \\ -0.7070 \\ -0.0060 \\ 0.7070 \\ 0.0000 \\ 0.0099 \\ 0.0060 \\ -0.0099 \\ 0.0000 \end{bmatrix}, \quad \boldsymbol{\phi}_3^* = \begin{bmatrix} 0.0197 \\ -0.7041 \\ -0.0039 \\ -0.7041 \\ -0.0892 \\ -0.0083 \\ -0.0039 \\ -0.0083 \\ 0.0013 \end{bmatrix}, \quad \boldsymbol{\phi}_4^* = \begin{bmatrix} -0.0049 \\ 0.0633 \\ 0.0062 \\ 0.0633 \\ -0.9941 \\ -0.0432 \\ 0.0062 \\ -0.0432 \\ 0.0003 \end{bmatrix}, \quad \boldsymbol{\phi}_5^* = \begin{bmatrix} 0.0000 \\ 0.0051 \\ -0.7040 \\ -0.0051 \\ 0.0000 \\ -0.0656 \\ 0.7040 \\ 0.0656 \\ 0.0000 \end{bmatrix}$$

$$\boldsymbol{\phi}_6^* = \begin{bmatrix} -0.0025 \\ -0.0048 \\ 0.7040 \\ -0.0048 \\ 0.0028 \\ 0.0615 \\ 0.7040 \\ 0.0615 \\ 0.0326 \end{bmatrix}, \quad \boldsymbol{\phi}_7^* = \begin{bmatrix} 0.0000 \\ 0.0105 \\ -0.0655 \\ -0.0105 \\ 0.0000 \\ 0.7040 \\ 0.0655 \\ -0.7040 \\ 0.0000 \end{bmatrix}, \quad \boldsymbol{\phi}_8^* = \begin{bmatrix} -0.0015 \\ 0.0039 \\ 0.0635 \\ 0.0039 \\ 0.0619 \\ -0.6987 \\ 0.0635 \\ -0.6987 \\ -0.1084 \end{bmatrix}, \quad \boldsymbol{\phi}_9^* = \begin{bmatrix} 0.0003 \\ 0.0015 \\ -0.0162 \\ 0.0015 \\ 0.0070 \\ -0.0782 \\ -0.0162 \\ -0.0782 \\ 0.9936 \end{bmatrix}.$$

The above vector components are given in the BFB $= \{w_{11}^*, w_{13}^*, w_{15}^*, w_{31}^*, w_{33}^*, w_{35}^*, w_{51}^*, w_{53}^*, w_{55}^*\}$.

(4) *Diagonal rigidity matrix for the first non-linear mode shape of FCRP with an aspect ratio α=1 expressed in MFB*

$$\left[\tilde{\mathbf{k}}_{ij}^*\right] = \begin{bmatrix} 1295.9230 & & & & & & & & & \\ & 17\,328.5273 & & & & & & & & \\ & & 17\,488.9860 & & & & & & & \\ & & & 148\,625.3226 & & & & & & \\ & & & & 95\,511.7737 & & & & & \\ & & & & & 95\,653.9895 & & & & \\ & & & & & & 155\,357.1090 & & & \\ & & & & & & & 156\,054.9693 & & \\ & & & & & & & & 319\,922.3785 \end{bmatrix}.$$

Appendix B. Details of numerical comparisons for a distributed force

B.1. The single-mode approximation in the BFB

$$(k_{11} - \omega^2 m_{11})q_1 + \tfrac{3}{2}b_{1111}q_1^3 = F_0 \sin \omega t \int_S w_1(x,y)\,\mathrm{d}x\mathrm{d}y. \tag{B.1}$$

In the present model

$$W_1(x,y,t) = Hw_1^*(x^*,y^*)q_1(t), \tag{B.2}$$

$$q_1(t) = a_1 \sin \omega t \tag{B.3}$$

which leads to

$$w_1(x,y) = Ha_1 w_1^*(x^*,y^*), \tag{B.4}$$

and

$$w_{max} = Ha_1 w_1^*\left(\tfrac{1}{2},\tfrac{1}{2}\right). \tag{B.5}$$

In the model presented in Ref. [30]:

$$w_1(x,t) = HAq(t)\phi(x,y), \tag{B.6}$$

so

$$w_{\max} = HA. \tag{B.7}$$

To compare the present results with those given in Ref. [30],

$$A = a_1 w_1^*\left(\tfrac{1}{2},\tfrac{1}{2}\right). \tag{B.8}$$

Eq. (B.1) can be written in non-dimensional form as

$$\left(\frac{DaH^2}{b^3}k_{11}^* - \omega^2 \rho H^3 abm_{11}^*\right)a_1 + \tfrac{3}{2}\,\frac{DaH^2}{b^3}b_{1111}^* a_1^3 = \alpha \tag{B.9}$$

Substituting the expression for the non-linear frequency $\omega^2 = \omega^{*2}D/\left(\rho Hb^4\right)$ in Eq. (B.9) leads to

$$\frac{DaH^2}{b^3}\left((k_{11}^* - \omega^{*2}m_{11}^*)a_1 + \tfrac{3}{2}b_{1111}^* a_1^3\right) = \alpha \tag{B.10}$$

The right-hand side of Eq. (B.10) can be expressed using non-dimensional parameters as follows:

$$k_{11}^* - \omega^{*2}m_{11}^* + \tfrac{3}{2}b_{1111}^* a_1^2 = \frac{F_0 b^4}{a_1 DH}\iint_{s^*} w_1^*(x^*,y^*)\mathrm{d}x^*\mathrm{d}y^* \tag{B.11}$$

which is equivalent to:

$$1 - \frac{\omega^{*2}}{\omega_l^{*2}} + \tfrac{3}{2}b_{1111}^*\frac{a_1^2}{k_{11}^*} = \frac{F_0 b^4}{a_1 DHk_{11}^*}\iint_{s^*} w_1^*(x^*,y^*)\mathrm{d}x^*\mathrm{d}y^* \tag{B.12}$$

which can also be written as

$$\left(\frac{\omega^*}{\omega_l^*}\right)^2 = 1 + \frac{3}{2}\frac{b_{1111}^*}{k_{11}^*}a_1^2 - \frac{f_1^*}{k_{11}^* a_1} \tag{B.13}$$

with

$$f_1^* = \frac{F_0 b^4}{DH}\iint_{s^*} w_1^*(x^*, y^*)\mathrm{d}x^*\mathrm{d}y^*. \tag{B.14}$$

In Ref. [30], the non-dimensional force P_0 is defined as

$$P_0 = \frac{cF_0}{\rho H^2\omega^2} \quad \text{with} \quad c = \frac{\iint \phi(x,y)\mathrm{d}x\mathrm{d}y}{\iint \phi^2(x,y)\mathrm{d}x\mathrm{d}y} \tag{B.15, 16}$$

in which ϕ is the normalized mode shape, and F_0 is the amplitude of the external applied force ($\mathrm{N/m^2}$). Combining Eqs. (B.4) and (B.6) leads to

$$\phi(x,y) = \frac{a_1}{A} w_1^*(x^*, y^*). \tag{B.17}$$

Substituting the expression for ϕ given in Eq. (B.17) into (B.16) gives:

$$\begin{aligned} P_0 &= \frac{cF_0}{\rho H^2\omega^2} = \frac{\iint \phi(x,y)\,\mathrm{d}x\,\mathrm{d}y}{\iint \phi^2(x,y)\,\mathrm{d}x\,\mathrm{d}y}\ \frac{F_0}{\rho H^2 \dfrac{D}{\rho H b^4}\omega^{*2}} = \frac{\dfrac{a_1}{A}\iint w_1^*\,\mathrm{d}x\,\mathrm{d}y}{\dfrac{a_1^2}{A^2}\iint w_1^{*2}\,\mathrm{d}x\,\mathrm{d}y}\ \frac{F_0 b^4}{HD\dfrac{k_{11}^*}{m_{11}^*}} \\ &= \frac{A}{a_1}\iint w_1^*\,\mathrm{d}x\,\mathrm{d}y \frac{F_0 b^4}{HDk_{11}^*} = \frac{A}{a_1}\ \frac{f_1^*}{k_{11}^*} = w_1^*\left(\tfrac{1}{2},\tfrac{1}{2}\right)\frac{f_1^*}{k_{11}^*}. \end{aligned} \tag{B.18}$$

B.2. The single-mode approximation in the MFB

In the same manner, to compare the present results with those of Ref. [30],

$$A = \bar{a}_1\phi_1^*\left(\tfrac{1}{2},\tfrac{1}{2}\right), \tag{B.19}$$

$$(\bar{k}_{11} - \omega^2\bar{m}_{11})\bar{q}_1 + \tfrac{3}{2}\bar{b}_{1111}\bar{q}_1^3 = F_0\sin\omega t\int_S \phi_1(x,y)\mathrm{d}x\mathrm{d}y. \tag{B.20}$$

Eq. (B.20) can be written in non-dimensional form as

$$\left(\frac{DaH^2}{b^3}\bar{k}_{11}^* - \omega^2\rho H^3 ab\bar{m}_{11}^*\right)\bar{a}_1 + \tfrac{3}{2}\ \frac{DaH^2}{b^3}\bar{b}_{1111}^*\bar{a}_1^3 = \bar{\alpha} \tag{B.21}$$

which is equivalent, if non-dimensional parameters are used, to

$$\bar{k}_{11}^* - \omega^{*2}\bar{m}_{11}^* + \tfrac{3}{2}\bar{b}_{1111}^*\bar{a}_1^2 = \frac{F_0 b^4}{\bar{a}_1 DH}\iint_{s^*}\phi_1^*(x^*, y^*)\mathrm{d}x^*\mathrm{d}y^* \tag{B.22}$$

which can be written as

$$\left(\frac{\omega^*}{\omega_1^*}\right)^2 = 1 + \tfrac{3}{2}\ \frac{\bar{b}_{1111}^*}{\bar{k}_{11}^*}\bar{a}_1^2 - \frac{\bar{f}_1^*}{\bar{k}_{11}^*\bar{a}_1} \tag{B.23}$$

with

$$\bar{f}_1^* = \frac{F_0 b^4}{DH} \iint_{s^*} \phi_1^*(x^*, y^*) \mathrm{d}x^* \mathrm{d}y^* \tag{B.24}$$

and

$$P_0 = \frac{cF_0}{\rho H^2 \omega^2} = \frac{\iint \phi(x,y)\ \mathrm{d}x\ \mathrm{d}y}{\iint \phi^2(x,y)\ \mathrm{d}x\ \mathrm{d}y} \frac{F_0}{\rho H^2 \dfrac{D}{\rho H b^4} \omega^{*2}} = \frac{\bar{a}_1 / A \iint \phi_1^*\ \mathrm{d}x\ \mathrm{d}y}{\bar{a}_1^2 / A^2 \iint \phi_1^{*2}\ \mathrm{d}x\ \mathrm{d}y} \frac{F_0 b^4}{HD \dfrac{\bar{k}_{11}^*}{\bar{m}_{11}^*}}$$

$$= \frac{A}{\bar{a}_1} \iint \phi_1^*\ \mathrm{d}x\ \mathrm{d}y \frac{F_0 b^4}{HD \bar{k}_{11}^*} = \frac{A}{\bar{a}_1} \frac{\bar{f}_1^*}{\bar{k}_{11}^*} = \phi_1^*\left(\tfrac{1}{2}, \tfrac{1}{2}\right) \frac{\bar{f}_1^*}{\bar{k}_{11}^*}. \tag{B.25}$$

Appendix C. Simply supported plates

The linear mode shapes for a simply supported rectangular plate are given by

$$w_{mn} = h \sin \frac{m\pi x}{a} \sin \frac{n\pi y}{b} \tag{C.1}$$

in which m and n are integers. The first mode shape, corresponding to $m = n = 1$ is given by

$$w_{11}(x,y) = h \sin \frac{\pi x}{a} \sin \frac{\pi y}{b} = h \sin \pi x^* \sin \pi y^*; \tag{C.2}$$

the associated non-dimensional mode is

$$w_{11}^*(x,y) = \sin \pi x^* \sin \pi y^*. \tag{C.3}$$

C.1. Expressions of the axial strain energy

If the in-plane displacements are taken into account, the expression for the axial strain energy is

$$V_a = \frac{3D}{2H^2} \int_S \left[\left(\frac{\partial W_1}{\partial x} \right)^2 + \left(\frac{\partial W_1}{\partial y} \right)^2 \right]^2 \mathrm{d}S = \frac{DaH^2}{b^3} \int_{S^*} \frac{3}{2} \left[\left(\alpha^2 \frac{\partial W_1^*}{\partial x^*} \right)^2 + \left(\frac{\partial W_1^*}{\partial y^*} \right)^2 \right]^2 \mathrm{d}S^* \tag{C.4}$$

from Eq. (6) in which $a_i = a_j = a_k = a_l = a_1 \sin \omega t$, we have

$$V_a = \tfrac{1}{2} a_1^4 b_{1111} \sin^4 \omega t \tag{C.5}$$

with

$$b_{1111}^* = \int_{S^*} 3 \left[\left(\alpha^2 \frac{\partial W_1^*}{\partial x^*} \right)^2 + \left(\frac{\partial W_1^*}{\partial y^*} \right)^2 \right]^2 \mathrm{d}S^{**}. \tag{C.6}$$

After substitution of Eq. (C.3) into (C.6), we obtain

$$b^*_{1111} = \frac{27\pi^4}{64}\left(\alpha^8 + \frac{8\alpha^4}{9} + 1\right). \tag{C.7}$$

C.2. Expression for the bending strain energy

The expression for the bending strain energy is given in Ref. [14]:

$$V_b = \frac{D}{2}\int_S \left[\left(\frac{\partial^2 W_1}{\partial x^2} + \frac{\partial^2 W_1}{\partial y^2}\right)^2 + 2(1-\nu)\left(\left(\frac{\partial^2 W_1}{\partial x \partial y}\right)^2 - \left(\left(\frac{\partial^2 W_1}{\partial x^2}\right)\left(\frac{\partial^2 W_1}{\partial y^2}\right)\right)\right) \mathrm{d}S\right] \tag{C.8}$$

using Eq. (C.2) and (C.8), one can easily obtain

$$V_b = \frac{DaH^2}{b^3}\int_{S^*} \frac{\alpha^4}{2}\left(\frac{\partial^2 W_1^*}{\partial x^{*2}}\right)^2 + \frac{1}{2}\left(\frac{\partial^2 W_1^*}{\partial y^{*2}}\right)^2 + (1-\nu)\alpha^2\left(\frac{\partial^2 W_1^*}{\partial x^* \partial y^*}\right)^2 + \nu\alpha^2\left(\frac{\partial^2 W_1^*}{\partial x^{*2}}\right)\left(\frac{\partial^2 W_1^*}{\partial y^{*2}}\right)\mathrm{d}x^*\,\mathrm{d}y^*. \tag{C.9}$$

Therefore

$$k^*_{11} = \int_{S^*} \alpha^4\left(\frac{\partial^2 W_1^*}{\partial x^{*2}}\right)^2 + \left(\frac{\partial^2 W_1^*}{\partial y^{*2}}\right)^2 + 2(1-\nu)\alpha^2\left(\frac{\partial^2 W_1^*}{\partial x^* \partial y^*}\right)^2 + 2\nu\alpha^2\left(\frac{\partial^2 W_1^*}{\partial x^{*2}}\right)\left(\frac{\partial^2 W_1^*}{\partial y^{*2}}\right)\mathrm{d}x^*\,\mathrm{d}y^*. \tag{C.10}$$

$$k^*_{11} = \frac{\pi^4}{2}(\alpha^2+1)^2. \tag{C.11}$$

for $\alpha = 1$, we have $k^*_{11} = 2\pi^4 \cong 194.8182$, and $b^*_{1111} = 39\pi^4/32 \cong 118.7028$.

Appendix D. Nomenclature

General notations

a,b	length, width of the plate
A	non-dimensional amplitude of vibration defined in the BFB by $A = a_1 w_1^*(C)$, and in the MFB by $A = \bar{a}_1 \phi_1^*(C)$
ANM	asymptotic-numerical method
BFB	beam function basis
c	a parameter defined by $c = \dfrac{\iint \phi(x,y)\mathrm{d}x\mathrm{d}y}{\iint \phi^2(x,y)\mathrm{d}x\mathrm{d}y}$ with $\phi(x,y)$ representing the normalized spatial function satisfying $\phi_{max} = 1$ [31].
C	plate centre
D	bending stiffness, $D = EH^3/12(1-\nu^2)$
E	Young's modulus

f_i^{*c}	dimensionless generalized force corresponding to concentrated force F^c
f_i^{*d}	dimensionless generalized force corresponding to distributed force F^d
F^c	concentrated harmonic force
F^d	distributed harmonic force
FCRP	fully clamped rectangular plate, or fully clamped rectangular plates, depending on the context
FEM	finite element method
H	thickness of the plate
HFEM	hierarchical finite element method.
[**M**], [**K**], [**B**]	mass matrix, linear rigidity matrix and non-linear rigidity matrix respectively
MFB	modal function basis
NLSSPFR	non-linear steady state periodic forced response
q_i	generalized co-ordinate $q_i(t) = a_i \sin(\omega t)$
S, S^*	dimensional and non-dimensional surfaces $[0,a] \times [0,b]$ and $[0,1] \times [0,1]$, respectively
T	kinetic energy
U and V	in-plane displacements in the x and y directions, respectively,
V_b, V_a and V	bending, axial and total strain energy, respectively
$W(x, y, t)$	transverse displacement at point (x,y) on the plate
$w_{ij}(x,y)$	basic function obtained as product of the ith clamped–clamped beam function in the x direction with the jth clamped–clamped beam function in the y direction
$W^*_{\omega^* l}(x^*, y^*, t)$	linear frequency response
$W^*_{\omega^* nl}(x^*, y^*, t)$	non-linear frequency response
(x,y)	point co-ordinates
$\bar{x}$	indicates parameters expressed in the MFB
*	the star exponent indicates non-dimensional parameters

Greek Letters

α	the plate aspect ratio $\alpha = b/a$
ε_r	basic function contribution
$\bar{\varepsilon}_r$	modal function contribution
v	the Poisson ratio
ρ	Mass density per unit volume of the plate
ϕ_i^*	ith linear mode shape
τ	Non-dimensional time parameter defined by $\tau = \omega t$
ω	Non-linear frequency
ω_L	Linear frequency

References

[1] R.G. White, Developments in the acoustic fatigue design process for composite aircraft structures, Composite Structures 16 (1990) 171–192.

[2] C. Mei, K.R. Wentz, Large-amplitude random response of angle-ply laminated composite plates, American Institute of Aeronautics and Astronautics Journal 20 (10) (1982) 1450–1458.
[3] R. Benamar, Non-linear Dynamic Behaviour of Fully Clamped Beams and Rectangular Isotropic and Laminated Plates, Ph.D.Thesis, University of Southampton, 1990.
[4] R. Benamar, M.M.K. Bennouna, R.G. White, The effects of large vibration amplitudes on the mode shapes and natural frequencies of thin elastic structures. Part I: simply supported and clamped–clamped beams, Journal of Sound and Vibration 149 (1991) 179–195.
[5] R. Benamar, M.M.K. Bennouna, R.G. White, The effects of large vibration amplitudes on the mode shapes and natural frequencies of thin elastic structures. Part II: fully clamped rectangular isotropic plates, Journal of Sound and Vibration 164 (1991) 399–424.
[6] R. Benamar, M.M.K. Bennouna, R.G. White, The effects of large vibration amplitudes on the fundamental mode shape of a fully clamped, symmetrically laminated, rectangular plate, Proceedings of the Fourth International Conference on Structural Dynamics: Recent Advances, Southampton, UK, 1991.
[7] M. El Kadiri, R. Benamar, R.G. White, The non-linear free vibration of fully clamped rectangular plates: second non-linear mode for various plate aspect ratios, Journal of Sound and Vibration 228 (2) (1999) 333–358.
[8] F. Moussaoui, R. Benamar, R.G. White, The effect of large vibration amplitudes on the mode shapes and natural frequencies of thin elastic shells. Part I: coupled transverse-circumferential mode shapes of isotropic circular shells of infinite length, Journal of Sound and Vibration 232 (5) (2000) 917–943.
[9] L. Azrar, R. Benamar, R.G. White, A semi-analytical approach to the non-linear dynamic response. Problem of S–S and C–C beams at large vibration amplitudes. Part I: general theory and application to the single mode approach to free and forced vibration analysis, Journal of Sound and Vibration 224 (2) (1999) 377–395.
[10] L. Azrar, R. Benamar, R.G. White, A semi-analytical approach to the non-linear dynamic response. Problem of beams at large vibration amplitudes. Part II: multimode approach to the forced vibration analysis, Journal of Sound and Vibration 255 (2002) 1–41.
[11] M. El. Kadiri, R. Benamar, R.G. White, Improvement of the semi-analytical method, based on Hamilton's principle and spectral analysis, for determination of the geometrically non-linear free response of thin straight structures Part I: application to c–c and ss–c beams, Journal of Sound and Vibration 249 (2) (2002) 263–305.
[12] M. El Kadiri, R. Benamar, R.G. White, Improvement of the semi-analytical method, based on Hamilton's principle and spectral analysis, for determination of the geometrically non-linear free response of thin straight structures. Part II: application to the first and second non-linear mode shapes of fully clamped rectangular plates, Journal of Sound and Vibration, submitted.
[13] R. Benamar, M.M.K. Bennouna, R.G. White, The effects of large vibration amplitudes on the mode shapes and natural frequencies of thin elastic structures. Part III: fully clamped rectangular isotropic plates-measurement of the mode shape amplitude dependence and spatial distribution of harmonic distortion, Journal of Sound and Vibration 175 (1991) 377–395.
[14] S. Timoshenko, S. Woinowsky-Krieger, Theory of Plates and Shells. 2nd Edition. McGraw-Hill, p. 345.
[15] B. Harras, R. Benamar, R.G. White, Experimental and theoretical investigation of the linear and non-linear dynamic behaviour of a Glare 3 hybrid composite panel, Journal of Sound and Vibration 252 (2) (2002) 281–315.
[16] B. Harras, R. Benamar, R.G. White, Geometrically non-linear free vibration analysis of fully clamped composite laminated plates. Part I: general theory, experimental and theoretical investigations of the fundamental non-linear mode shape, Journal of Sound and Vibration 251 (4) (2002) 579–619.
[17] B. Harras, R. Benamar, R.G. White, Investigation of non-linear free vibrations of fully clamped symmetrically laminated carbon-reinforced-PEEK (AS4/APC2) rectangular panels, Composites Science and Technology 62 (2002) 719–727.
[18] F. Moussaoui, R. Benamar, R.G. White, The effects of large vibration amplitudes on the mode shapes and natural frequencies of thin elastic shells. Part II: a new approach for free transverse constrained vibration of cylindrical shells, Journal of Sound and Vibration 255 (5) (2002) 931–963.
[19] B. Nageswara Rao, S.R.R. Pillai, Exact solution of the equation of motion to obtain non-linear vibration characteristics of thin plates, Journal of Sound and Vibration 153 (1) (1992) 168–170.
[20] D.J. Ewins, Modal Testing, Theory and Practice, Research Studies Press, 1984.
[21] F. Moussaoui, R. Benamar, R.G. White, Authors' reply, Journal of Sound and Vibration 243 (1) (2001) 184–189.

[22] H. Vold, Insight, not numbers, in: Proceedings of the seven International Modal Analysis Conference, Las Vegas, Nevada, 1989.
[23] A.V. Srinivasan, Non-linear vibrations of beams and rectangular plates, International Journal of Non-linear Mechanics 1 (1966) 179–191.
[24] B. Bharat, G. Singh, G. Venkateswara Rao, An iteration method for the large amplitude flexural vibration of anti-symmetric cross-ply rectangular plates, Composite Structures 18 (1991) 263–282.
[25] P.C. Dumir, A. Bhaskar, Some erroneous finite element formulations of non-linear vibrations of beams and plates, Journal of Sound and Vibration 123 (3) (1988) 517–527.
[26] C.S. Hsu, On the application of elliptic functions in non-linear forced oscillations, Quarterly Journal of Applied Mathematics 17 (1960) 393–407.
[27] J.G. Eisley, Non-linear vibrations of beams and rectangular plates, Zeitschrift für Angewandte Mathematik und Physik 15 (1964) 167–175.
[28] J.J. Stoker, Non-linear Vibrations, Interscience, New York, 1950.
[29] S. Wang, K. Huseyin, Maple analysis of non-linear oscillations, Mathematica Computing and Modelling 16 (1992) 49–57.
[30] C. Mei, K. Decha-Umphai, A finite element method for non-linear forced vibrations of rectangular plates, American Institute of Aeronautics and Astronautics Journal 23 (7) (1985) 1104–1110.
[31] P. Ribeiro, M. Petyt, Non-linear vibration of plates by the hierarchical finite element and continuation methods, International Journal of Mechanical Sciences 41 (1999) 437–459.
[32] L. Azrar, E.H. Boutyour, M. Potier-Ferry, Non-linear forced vibrations of plates by an asymptotic numerical method, Journal of Sound and Vibration 252 (4) (2002) 657–674.
[33] W. Han, M. Petyt, Geometrically non-linear vibration analysis of thin, rectangular plates using the hierarchical finite element method — I: the fundamental mode of isotropic plates, Computers and Structures 63 (2) (1997) 295–308.
[34] S. Rao, A. Sheikh, M. Mukhopadhyay, Large-amplitude finite element flexural vibration of plates/stiffened plates, Journal of Acoustical Society America 93 (6) (1993) 3250–3257.